NON-LINEAR OSCILLATION OF SYNCHRONOUS MACHINE

A Dissertation
submitted in partial fulfilment
of the requirements for the Degree
of
MASTER OF ENGINEERING
in
ADVANCED ELECTRICAL MACHINES

By

S. K. MURTHY

DEPARTMENT OF ELECTRICAL ENGINEERING
UNIVERSITY OF ROORKEE
ROORKEE

July, 1968

CERTIFICATE

Certified that the dissertation entitled "NON-LINEAR OSCILLATION OF SYNCHRONOUS MACHINE" being submitted by Sri S. Keshava Murthy in partial fulfilment for the award of the degree of Master of Engineering in Advanced Electrical Machines of the University of Roorkee is a record of the student's own work carried out by him under my supervision and guidance. The matter embodied in this dissertation has not been submitted for the award of any other degree or diploma.

This is further to certify that he has worked for a period of 7 months from January 1, 1968 to July 31,1968 for preparing this dissertation for Master of Engineering degree at the University.

Dated: 3.8.68.

P. Mukhopadhyay

Dr. P. Mukhopadhyay,
Professor of Electrical Engg.,
University of Roorkee,
R o o r k e e

ACKNOWLEDGEMENT

The author expresses his deep gratitude for Dr. P. Mukhopadhyay, Professor of Electrical Engineering at the University of Roorkee for the good guidance and kind assistance accorded to him at every stage of the work connected with this dissertation.

He sincerely thanks the Head of the Department of Electrical Engineering for kindly extending every facility in the department in connection with this work.

Thanks are due to Dr. L.M. Ray, Professor of Electrical Engineering, for permitting the author to do whatever modification was necessary in the machines concerned. The staff of the Electrical Engineering Workshop will ever be remembered for their readiness at and accuracy in the work involving fitting and fabrication of different devices. He thanks Sri S.K. Jain, Reader in Electrical Engineering for promptly arranging for stabilised D.C. supply throughout the period of experimental investigation.

He would finally thank every body who has directly or otherwise influenced his work.

C_O_N_T_E_N_T_S

NOMENCLATURE

ψ	.. Flux linkage
i, I	.. Current, R.M.S. value
x	.. Steady State reactance
$x(jK)$	.. Operational impedance at frequency K
K	.. Oscillation periodicity
$\frac{K}{2\pi}$	.. Oscillation frequency
$f, \frac{w}{2\pi}$	.. Synchronous or line frequency
w	.. Synchronous periodicity, Synchronous Speed, elect.rad./sec.
ν	.. Actual, instantaneous speed, elect.rad./sec.
p	.. Derivative operator, $\frac{d}{dt}$
b	.. Ratio $\frac{x_d}{x_q}$
t	.. Time, sec.
δ	.. Instantaneous load angle, elect.rad.or degree.
θ	.. Instantaneous angular position of the rotor, degree Angle of torsional twist in a shaft, mech.rad.or degree.
e, V	.. Terminal voltage, R.M.S. value.
E_o	.. Maximum value of excitation e.m.f.
T	.. Torque
r	.. Resistance
x_l	.. Armature leakage reactance
x_{ad}	.. Direct axis armature reaction reactance,
x_{aq}	.. Quadrature axis armature reaction reactance,
P	.. Power, watts
T'_{do}	.. Open circuit transient time constant, d-axis.
T'_d	.. Short circuit transient time constant, d-axis
Z_{in}	.. Input impedance
G	.. Modulus of rigidity
a.c.	.. Alternating current

d.c.	..	Direct current
o.c.	..	Open circuit
s.c.	..	Short circuit
c.p.s.	..	Cycles per sec.
C.R.O.	..	Cathode Ray Oscillograph
D.O.	..	Duddell Oscillograph

SUFFIXES:

d	..	Direct axis
q	..	Quadrature axis
s	..	Sine component
c	..	Cosine component
n	..	Harmonic order
d(q)	..	direct or quadrature axis
s(c)	..	Sine or Cosine component
o	..	Average value
m	..	Maximum value
kd	..	Direct axis damper
kq	..	Quadrature axis damper
f	..	Main field

S_U_M_M_A_R_Y.

Application of the small oscillation theory for studying self and forced oscillations in a synchronous machine is well known. If the oscillation is large this linear theory loses its validity since the current, voltage and torque no longer vary proportionately. The machine oscillation is then classified as non-linear. Here is an attempt to analyse a large nonlinear oscillation and to determine the torque variation resulting from a known load angle variation of large amplitude. Park's equations of the d-q axes voltages are rigorously solved for the axes flux linkages, the axes voltages are expanded into infinite series using Bessel's functions and the flux linkage co-efficients are written down. Using operational impedances current coefficients are calculated and finally torque is evaluated.

Constants of a laboratory synchronous machine are determined accurately. Using the analysis developed its torque is computed for a large load-angle oscillation of low frequency.

Attempt is also made to develop an experimental technique to verify the validity of the large oscillation theory. As a requirement, a load angle recording device, a low-frequency oscillation-generating device and a torque recording device are designed using simple principles, and constructed. Using these apparatus an experimental set-up is arranged to record the torque and current variation for a known load angle variation. Measuring from the oscillograms the departure or otherwise of the torque and/or current from the theoretically estimated value is graphically represented.

CHAPTER I

INTRODUCTION:

The characteristics of a synchronous machine that its stator-rotor electro-magnetic coupling is elastic and that the rotor possesses inertia render the synchronous machine an oscillating system. These oscillations are electromechanical in nature since torque is produced owing to interaction between flux and current defining an electrical character, and the rotor inertia, shaft elasticity and friction constitute a mechanical character. A comprehensive analysis based on both is so far not done to the best knowledge of the author. Excellent piece-meal works are available.

Park's two-reaction theory has been used to determine the influence of the circuit parameters on the torque developed under oscillating conditions. Two papers[1,2] appeared in 1930 in Transactions A.I.E.E. fully analysing the effect of armature circuit resistance on hunting using the theory of small oscillations. W.J. Gibbs[3] in 1951 gave the 'matrix method' and B. Adkins[4] in 1957 gave a method for calculating the synchronising and damping torque co-efficients under oscillating conditions for a small-load angle variation and developed an experimental method in 1960. All these methods are applicable as long as the oscillations are small and can not be used once they are large because the change, then, in torque for a change in load angle is disproportionate.

The work presented here analyses large oscillations of low frequency lying between 0.5 cps to 2 cps. This frequency band is usually the one met with in practice when a synchronous machine hunts.[4,5] Analysis here is restricted to forced oscillations only. Commencing from Park's equations the theory is developed. Certain assumptions, as usual, are made.

A salient pole synchronous machine of 7.5 KW is used for the experimental investigation and its constants are carefully determined. Potier reactance method is used to determine x_1; maximum reluctance power test[6] is performed to calculate x_d and x_q; transient time constants T'_{do} and T'_d are found out from the oscillograms of armature voltage and armature short circuit current obtained when its field is suddenly short-circuited; using these time constants x_f and r_f are evaluated; finally, d-q axes operational impedances are measured at the synchronous frequency from which are computed the damper constants, r_{kd}, x_{kd}, r_{kq} and x_{kq}.

These constants are used to determine numerically the torque developed under oscillating conditions using the large oscillation theory developed here.

The work would be incomplete without an attempt for experimental verification, at least qualitatively. A set-up is, therefore, arranged with the necessary instrumentation designed and constructed. The instrumentation covers (i) a torque recording device[7] based on magnetic coupling technique which does away with the brushes and slip rings of conventional designs, (ii) a load angle recording device[5] based on the Z-modulation technique of the Cathode Ray beam of a C.R.O. with the conventional complex electronic circuitry being replaced by simple transistor pulse generators and (iii) a device for producing forced sinusoidal oscillations of low frequency using the simple mechanical technique of converting the rotary motion into reciprocatory motion.

Most often in the field one would encounter with the problem of large oscillations. Small oscillation theory is a mere mathematical expediency with its drastic limitations of applicability to linear cases only. It is hoped that the dissertation presented here provides a method useful for the analysis of nonlinear oscillations.

CHAPTER II

THEORY OF LARGE OSCILLATION

2.1. BRIEF REVIEW:

Short circuits and faults in power systems of which synchronous machines form a part, set up torque variations in the synchronous machines. The high frequency component as well as the d.c. component fall off rapidly to zero while the slowly varying component constitutes an important influence. It causes the rotor angle to swing and thus plays a decisive role in determining the transient stability of the system.

The problem of torque variation and load angle swing has been studied from time to time by the method of small oscillations. Dr. Ludwig Dreyfus has shown that sustained cumulative oscillations can occur without the presence of periodic exciting torque provided the conditions in the machine circuits are favourable. Nickle and Pierce[1] have estimated quantitatively that the damping torque of any synchronous machine would become negative giving rise to instability if the armature circuit resistance is increased beyond a critical limiting value. This value for a salient pole generator with normal excitation and no damper is-

$$r = x_q \tan\delta$$

The damping of a generator increases in the positive direction with the increase of load and a generator stable at no load remains stable under any steady load within the steady state stability limit. A generator can be made unstable by too much resistance in the armature circuit.

Adkins[4,5] deduced that synchronising (K) and damping (C) torque coefficients can be determined from the complex number

$$\frac{\Delta T}{\Delta \delta} = K+jmC = \frac{EV}{x_d}\cos\delta_o + V^2\left\{\frac{1}{x_q(jm)} - \frac{1}{x_d}\right\}\cos^2\delta_o + V^2\left\{\frac{1}{x_d(jm)} - \frac{1}{x_q}\right\}\sin^2\delta_o$$

as the real and imaginary parts of this equations. An experimental set up was developed to calculate K and C from the oscillograms of torque and load angle oscillations. S.B. Crary[27] derived, an approximate equation for C with certain approximations from Park's equations- as,

$$C = V^2\left\{\left(\frac{1}{x_d''} - \frac{1}{x_d'}\right)T_d'' \sin^2\delta_o + \left(\frac{1}{x_q''} - \frac{1}{x_q}\right)T_q'' \cos^2\delta_o\right\}$$

All these methods are based on the small oscillation theory.

For the first time an analysis of a large oscillation of low frequency, both self and forced, has been done by S. Basu and P. Mukherji.[8] In common with the other authors, Park's equations are used. The axes voltages are expanded into infinite series using Bessel's functions and the flux linkages are expressed as fourier series. Substituting these into Park's equations a set of equations for flux linkages is determined. Approximate solutions are written down since the number of unknowns is more by one than the number of equations, the difficulty of indeterminacy is obviated by assuming that the oscillation frequency is too small in comparison with the line frequency. The axes currents are calculated using the operational impedances and torque is evaluated. A numerical analysis using standard machine constants is made bringing out the difference between the small and large oscillation theories. No experimental analysis, however, is made.

The present dissertation proceeds on similar lines with certain differences as pointed out in Chapter I.

2.2. THEORY:

When a synchronous machine oscillates with a large amplitude it is interesting to be able to calculate the torque resulting from a large load angle variation. Park's equations of the d- q axes are rigorously solved as simultaneous equations in two unknowns, Ψ_d and Ψ_q; axes voltages are expanded into infinite series with the help of Bessel's functions and the flux linkage coefficients (average, sine and cosine components of the fundamental and various harmonics) are determined. Operational impedances $x_d(jnk)$ and $x_q(jnk)$ are calculated using the classical method of equivalent circuits, and the currents i_d, i_q (average, sine and cosine components of the fundamental and various harmonics) are computed using the basic relation,

$$\text{Current} = \frac{\text{w times the flux linkage coefficient}}{\text{the respective operational impedance}}$$

Electromagnetic torque is then calculated from the fundamental relation,

$$\text{Torque} = \frac{w}{2}\,(i_d\,\Psi_q - i_q\Psi_d).$$

2.3. ASSUMPTIONS:

The development of the theory is based on the following assumptions:

(i) The machine is connected to a relatively large power system so that when it hunts the bus bar voltage remains substantially constant; in other words, the machine is connected to an infinite bus.

(ii) Sinusoidal balanced voltages are applied to the stator and sinusoidal balanced currents flow in it; this makes the usual vector diagrams of voltages and currents per phase to be still valid.

(iii) The machine is in a state of sustained oscillations about a constant average value of the load angle; the fundamental component of the electromagnetic torque is a function of time and has two components, (a) one in time phase with the angular velocity of oscillation and (b) the other in time phase with the angular displacement; (a) is called "the damping torque" and (b) "the synchronising torque".

(iv) The oscillation frequency is small in comparison with the line frequency; thus torque and power are numerically equal in the per unit system.

(v) The load angle variation is sinusoidal; this is justified because the harmonics, particularly the higher ones, produced by the harmonic torque variations are smoothed out by the rotor inertia; a torque variation causes the load angle to vary and this load angle variation again affects the torque; the system is therefore cumulatively complex and a simple solution to the problem of oscillations of such a system is well nigh impossible. Hence, within reasonable limits the load angle is assumed to vary sinusoidally over a steady average value. Stated mathematically,

$$\delta = \delta_o + \delta_m \sin kt$$

(vi) Armature resistance and saturation are neglected.

2.4. ANALYSIS:

Park's equations of axes voltages are,

$$p\,\psi_d + \nu\,\psi_q = e_d \qquad \ldots (1)$$

$$-\nu\,\psi_d + p\,\psi_q = e_q \qquad \ldots (2)$$

But $\nu = p\theta$ ... ... (3)

and $\theta = wt - \delta$ ... ... (4)

Thus $\nu = w - p\delta$ ... ... (5)

Substituting (5) in (1) and (2)

$$p\,\psi_d + (w - p\delta)\,\psi_q = e_d \qquad \ldots (6)$$

$$-(w - p\delta)\,\psi_d + p\,\psi_q = e_q \qquad \ldots (7)$$

Multiplying (6) by $(w - p\delta)$ and (7) by p and adding,

$$\{(w-p\delta)^2 + p^2\}\,\psi_q = (w - p\delta)e_d + pe_q \qquad \ldots (8)$$

Thus,

$$\psi_q = \frac{(w - p\delta)\,e_d + pe_q}{(w - p\delta)^2 + p^2} \qquad \ldots (9)$$

and

$$\psi_d = \frac{pe_d - (w - p\delta)\,e_q}{(w - p\delta)^2 + p^2} \qquad \ldots (10)$$

Substituting,

$$e_d = e_m \sin\delta \quad \ldots \qquad \ldots (11)$$

$$e_q = e_m \cos\delta \quad \ldots \qquad \ldots (12)$$

in (9) and (10)

$$\psi_q = \frac{we_m \sin\delta - e_m \sin\delta\,(p\delta) - e_m \sin\delta\,(p\delta)}{w^2 - 2w(p\delta) + (p\delta)^2 + p^2}$$

$$= \frac{(w - 2p\delta)\,e_m \sin\delta}{w\,(w - 2p\delta)}$$

$$= \frac{e_m \sin\delta}{w} \quad \ldots \qquad \ldots (13)$$

and $$\psi_d = -e_m \frac{\cos\delta\,(w - 2p\delta)}{w\,(w - 2p\delta)}$$

$$= \frac{-e_m \cos\delta}{w} \quad \ldots \qquad \ldots (14)$$

since $$p^2 = -(p\delta)^2 \qquad \ldots (15)$$

Hence the rigorous solution of equations (1), (2) is

$$w\,\psi_d = -e_q \quad \ldots \qquad \ldots (16)$$

$$w\,\psi_q = e_d \quad \ldots \qquad \ldots (17)$$

Strangely enough the exact solutions (16) and (17) can also be obtained as approximate solutions by neglecting the transformer voltages in (1) and (2).

Substituting $\delta = \delta_o + \delta_m \sin Kt$ ... (18)

in (11) and (12),

$$e_d = e_m \sin \{ \delta_o + \delta_m \sin Kt \} \quad \ldots (19)$$

$$e_q = e_m \cos \{ \delta_o + \delta_m \sin Kt \} \quad \ldots (20)$$

Expanding with the help of Bessel's functions,

$$e_d = e_m \{ \sin \delta_o . \cos(\delta_m \sin Kt) + \cos \delta_o . \sin(\delta_m \sin Kt) \} \quad (21)$$

$$= e_m \sin \delta_o \left[J_o(\delta_m) + 2\{ J_2(\delta m) \cos 2Kt + J_4(\delta_m) \cos 4Kt + \ldots \ldots \} \right] + e_m \cos \delta_o \, 2\{ J_1(\delta_m) \sin Kt + J_3(\delta_m) \sin 3Kt + \ldots \} \quad \ldots (22)$$

and $e_q = e_m \cos \delta_o \cos(\delta_m \sin Kt) - e_m \sin \delta_o \sin(\delta_m \sin Kt)$. (23)

$$= e_m \cos \delta_o \left[J_o(\delta_m) + 2\{ J_2(\delta_m) \cos 2Kt + J_4(\delta_m) \cos 4Kt + \ldots \} \right] - e_m \sin \delta_o \, 2\{ J_1(\delta_m) \sin Kt + J_3(\delta_m) \sin 3Kt + \ldots \} \quad (24)$$

Thus (16), (17) with (22), (24) yield the following results for the flux linkage coefficients:

$$\Psi_{do} = - \frac{e_m \cos \delta_o J_o(\delta_m)}{w} \quad \ldots (25)$$

$$\Psi_{qo} = \frac{e_m \sin \delta_o J_o(\delta_m)}{w} \quad \ldots (26)$$

$$\Psi_{ds1} = \frac{2J_1(\delta_m) \, e_m \sin \delta_o}{w} \quad \ldots (27)$$

$$\Psi_{qs1} = \frac{2 J_1(\delta m) \, e_m \cos \delta_o}{w} \quad \ldots (28)$$

$$\Psi_{dc1} = 0 \quad \ldots \quad \ldots (29)$$

$$\Psi_{qc1} = 0 \quad \ldots \quad \ldots (30)$$

$$\Psi_{ds2} = 0 \quad \ldots \quad \ldots (31)$$

$$\psi_{qs2} = 0 \qquad \ldots \qquad \ldots (32)$$

$$\psi_{dc2} = -\frac{2\ J_2(\delta_m)\ e_m \cos\delta_o}{w} \qquad \ldots (33)$$

$$\psi_{qc2} = \frac{2\ J_2\ (\delta_m)\ e_m \sin\delta_o}{w} \qquad \ldots (34)$$

$$\psi_{ds3} = \frac{2\ J_3\ (\delta_m)\ e_m \sin\delta_o}{w} \qquad \ldots (35)$$

$$\psi_{qs3} = \frac{2\ J_3\ (\delta_m) e_m \cos\delta_o}{w} \qquad \ldots (36)$$

$$\psi_{dc3} = 0 \qquad \ldots \qquad \ldots (37)$$

$$\psi_{qc3} = 0 \qquad \ldots \qquad \ldots (38)$$

$$\psi_{ds4} = 0 \qquad \ldots \qquad \ldots (39)$$

$$\psi_{qs4} = 0 \qquad \ldots \qquad \ldots (40)$$

and so on.

Writing the most general terms,

$$\psi_{d(q)s2n} = 0 \qquad \ldots \qquad \ldots (41)$$

$$\psi_{d(q)c\ \overline{2n+1}} = 0 \qquad \ldots \qquad \ldots (42)$$

$$\psi_{ds\ \overline{2n+1}} = \frac{2J_{2m+1}(\delta_m)\ e_m \sin\delta_o}{w} \qquad \ldots (43)$$

$$\psi_{qs\ \overline{2n+1}} = \frac{2\ J_{2n+1}(\delta_m)\ e_m \cos\delta_o}{w} \qquad \ldots (44)$$

$$\psi_{dc\ 2n} = \frac{-2\ J_{2n}\ (\delta_m)\ e_m \cos\delta_o}{w} \qquad \ldots (45)$$

$$\psi_{qc\ 2n} = \frac{2\ J_{2n}\ (\delta_m)\ e_m \sin\delta_o}{w} \qquad \ldots (46)$$

From these equations it is evident that even sine and odd cosine terms do not exist among the flux linkage coefficients

2.5. CURRENTS:

Currents are calculated from-

$$\psi_d = x_d(p)\ i_d - G(p)\ e_{fd} \qquad \ldots (47)$$

$$\psi_q = -x_q(p)\ i_q \qquad \ldots (48)$$

The average terms are given by,

$$w\,\psi_{do} = x_d\, i_{do} - E_o \quad \ldots \quad \ldots (49)$$

$$w\,\psi_{qo} = x_q\, i_{qo} \quad \ldots \quad \ldots (50)$$

so that,

$$i_{do} = \frac{w\,\psi_{do} + E_o}{x_d} \quad \ldots \quad \ldots (51)$$

$$i_{qo} = \frac{w\,\psi_{qo}}{x_q} \quad \ldots \quad \ldots \quad \ldots (52)$$

and the Sine and Cosine terms at the oscillation frequency are,

$$i_{d(q)sn} = \frac{w\,\psi_{d(q)sn}}{x_{d(q)}(jnk)} \quad \ldots (53)$$

$$i_{d(q)cn} = \frac{w\,\psi_{d(q)cn}}{x_{d(q)}(jnk)} \quad \ldots \quad \ldots (54)$$

2.6. TORQUE:

Electromagnetic torque is calculated from-

$$T = \frac{W}{2}\,(i_d\,\psi_q - i_q\psi_d) \quad \ldots \quad \ldots (55)$$

Expanding,

$$T = \frac{W}{2} \left\{ i_{do} + \sum i_{dsn} \sin nkt + \sum i_{dcn} \cos nkt \right\}$$
$$\left\{ \psi_{qo} + \sum \psi_{qs\,\overline{2n+1}} \sin \overline{2n+1}\,kt + \sum \psi_{qc2n} \cos 2nkt \right\}$$
$$\left\{ i_{qo} + \sum i_{qsn} \sin nkt + \sum i_{qcn} \cos nkt \right\}$$
$$\left\{ \psi_{do} + \sum \psi_{ds\,\overline{2n+1}} \sin \overline{2n+1}\,kt + \sum \psi_{dc2n} \cos 2nkt \right\}$$
$$\ldots (56)$$

Summation being carried over from n=1 to $n = \infty$.

CHAPTER III

DETERMINATION OF MACHINE CONSTANTS

3.1. Choice, desirably, shall fall on the largest synchronous machine available. A 3-phase, 4 pole, 7.5 KVA, 400 Volt, 10.8Amps. 50 cps, revolving armature type, salient pole synchronous machine is chosen. It carries on its shaft a 40 volt, 0.35 kw 8.7A, shunt exciter and is driven by a 220Volt, 42A, 8KW, d.c. shunt motor. The constants to be determined are x_1, x_d, x_q, r_f, x_f, r_{kd}, x_{kd} and r_{kq}, x_{kq} so that using standard equivalent circuits[9] operational impedances at the oscillation frequencies may be computed. Standard accepted tests are conducted with the best possible accuracy.

3.2. DETERMINATION OF x_1:

Open circuit, short circuit and zero power factor full load tests are performed and the characteristics are plotted in Graph 3.1 and x_1 is scaled to be 0.122 p.u.

3.3. DETERMINATION OF x_d AND x_q:

A test known as Maximum Reluctance Power test[6] is performed. The synchronous machine is synchronised with the infinite bus and with its excitation reduced to zero it is loaded gradually by increasing the load on the d.c. machine now running as a generator. Voltage current and power input to the synchronous machine are measured at the instant at which the machine suffers loss of synchronism and runs as an induction motor as the load on it is increased. This significant instant is precisely recognised by using a good quality stroboscope triggered from the line frequency to which the synchronous machine is bound.

From the vector diagram of the synchronous machine as a motor, Fig.(3.2), under maximum reluctance power,

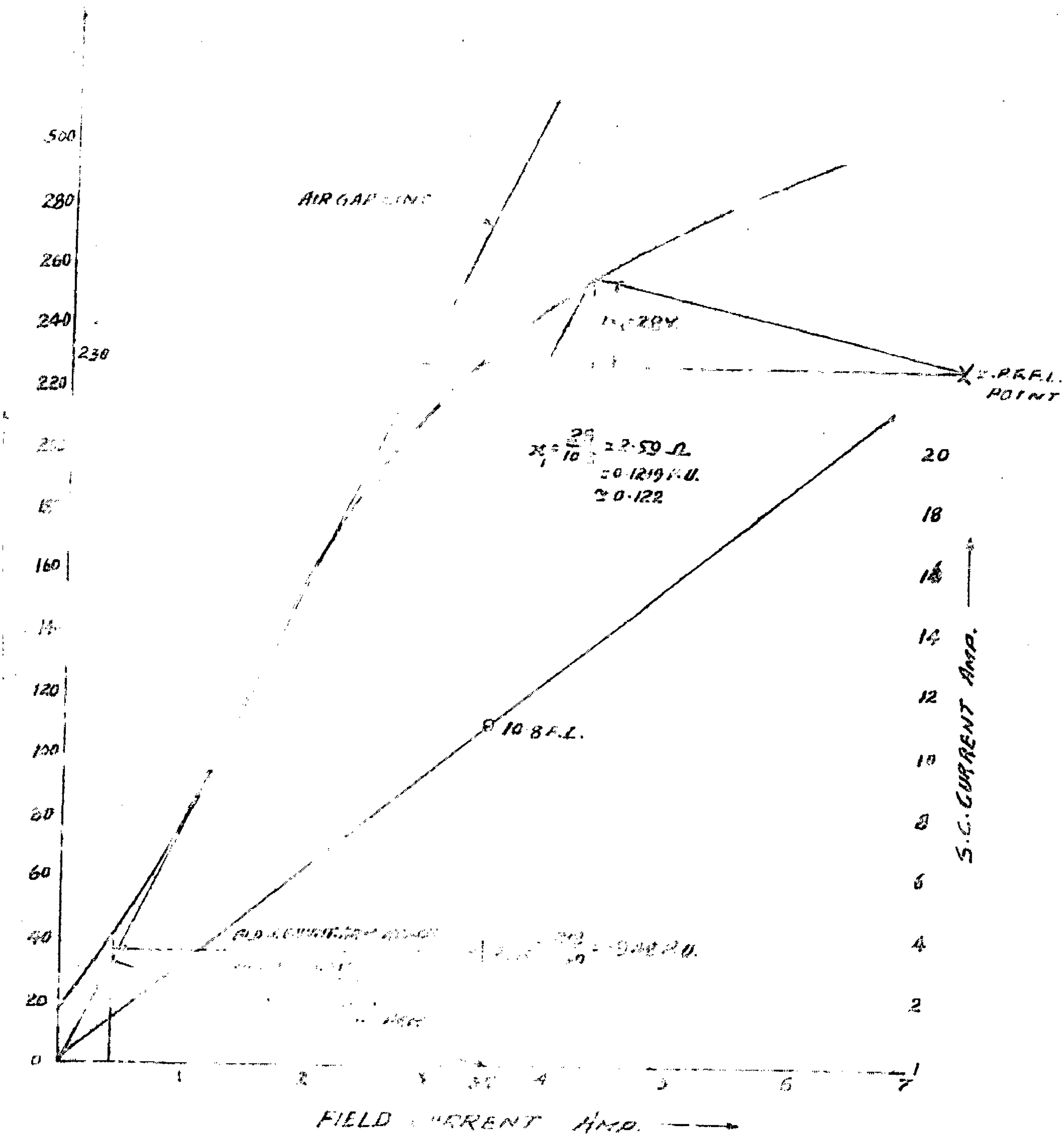

GRAPH FIG 31 DETERMINATION OF X_1

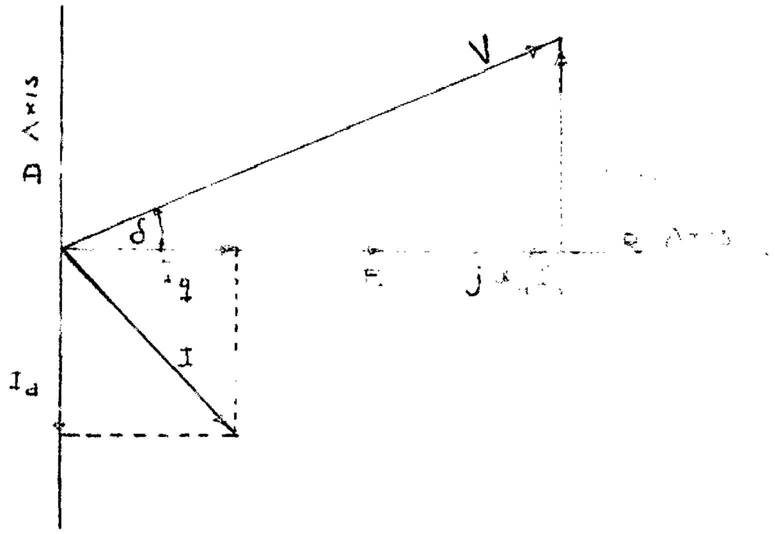

Fig. 3.2.

Vector diagram of Synch. Motor

$$E = 0, \quad \delta = 45^{\circ} \quad \text{so that}$$

$$V = jx_d I_d + jx_q I_q$$

$$\doteq V \cos\delta + jV \sin\delta \qquad \ldots \qquad \ldots(57)$$

$$\text{Thus} \quad x_d I_d = x_q I_q = \frac{V}{\sqrt{2}} \qquad \ldots \qquad \ldots(58)$$

$$\text{Also} \qquad I^2 = I_d^2 + I_q^2 \qquad \ldots \qquad \ldots(59)$$

$$I = \frac{V}{\sqrt{2}} \left(\frac{1}{x_d^2} + \frac{1}{x_q^2}\right)^{\frac{1}{2}} \qquad \ldots \qquad \ldots(60)$$

$$= \frac{V}{\sqrt{2}} \quad \frac{1}{x_q}\left(\frac{1 + b^2}{b^2}\right)^{\frac{1}{2}} \text{ where } b = \frac{x_d}{x_q} > 1 \ \ldots \qquad \ldots(61)$$

Maximum Power developed per phase is,

$$P_m = \frac{V^2}{2}\left(\frac{1}{x_q} - \frac{1}{x_d}\right) \qquad \ldots \qquad \ldots \qquad \ldots(62)$$

$$= \frac{V^2}{2x_q}\left(\frac{b-1}{b}\right) \qquad \ldots \qquad \ldots \qquad \ldots(63)$$

Dividing (63) by (61),

$$\frac{\sqrt{2} \; P_m}{VI} = \frac{b-1}{\sqrt{b^2+1}} \qquad \ldots \qquad \ldots \qquad \ldots(64)$$

$$\text{Letting} \quad a = \frac{\sqrt{2} \; P_m}{IV}, \quad ..$$

$$b^2 (1-a^2) - 2b + (1-a^2) = 0 \qquad \ldots \qquad \ldots(65)$$

from which b can be found as that root greater than 1. Substituting this value of b in (61), x_q is found and later x_d is found as bx_q.

Test results	Current,	18.4 Amps.
per phase are,	Voltage,	230 Volts
	Power,	1660 Watts.

Equation (65) will be-

$$b^2 - 2.83b + 1 = 0$$

whose solution is b =2.415

From (61), $x_q = 9.51$ ohm

and $x_d = 23.00$ ohms.

Base Impedance being, $\frac{230}{10.8} = 21.3$ ohms,

$x_d = 1.08$ P.U.

$x_q = 0.448$ P.U.

so that $x_{ad} = x_d - x_1 = 0.958$ P.U.

$x_{aq} = x_q - x_1 = 0.326$ P.U.

3.4. DETERMINATION OF x_f, r_f:

Equations[10]
$$\frac{1}{wr_f}(x_{ad} + x_f) = T'_{do} \quad \ldots (66)$$

$$\frac{1}{wr_f}\left(x_f + \frac{x_{ad} \cdot x_1}{x_{ad} + x_1}\right) = T'_d \quad \ldots (67)$$

are used to calculate x_f and r_f ~~by~~ knowing T'_{do} and T'_d. T'_{do} and T'_d are determined from the oscillograms of armature O.C. voltage and S.C. current which would decay exponentially to the values fixed by the residual field while the field winding is short circuited on itself. A Duddell oscillograph is used to record the transients. The field winding is connected in series with the make contacts of its A relay so that field short circuit takes place just at the instant at which the camera shutter opens as the shutter release button is pressed. Figs. (3.3) and (3.4) show the connections and Figs.(3.5) and (3.6) the oscillograms. Fig.(3.7) shows the plot of peaks of Figs.(3,4) versus time in milliseconds. T'_{do} and T'_d are read from the graphs in Fig.(3.7) to be the times for 0.368 of the initial values disregarding the initial decrement due to the first transient. Results are,

$T'_{do} = 1.1$ sec.

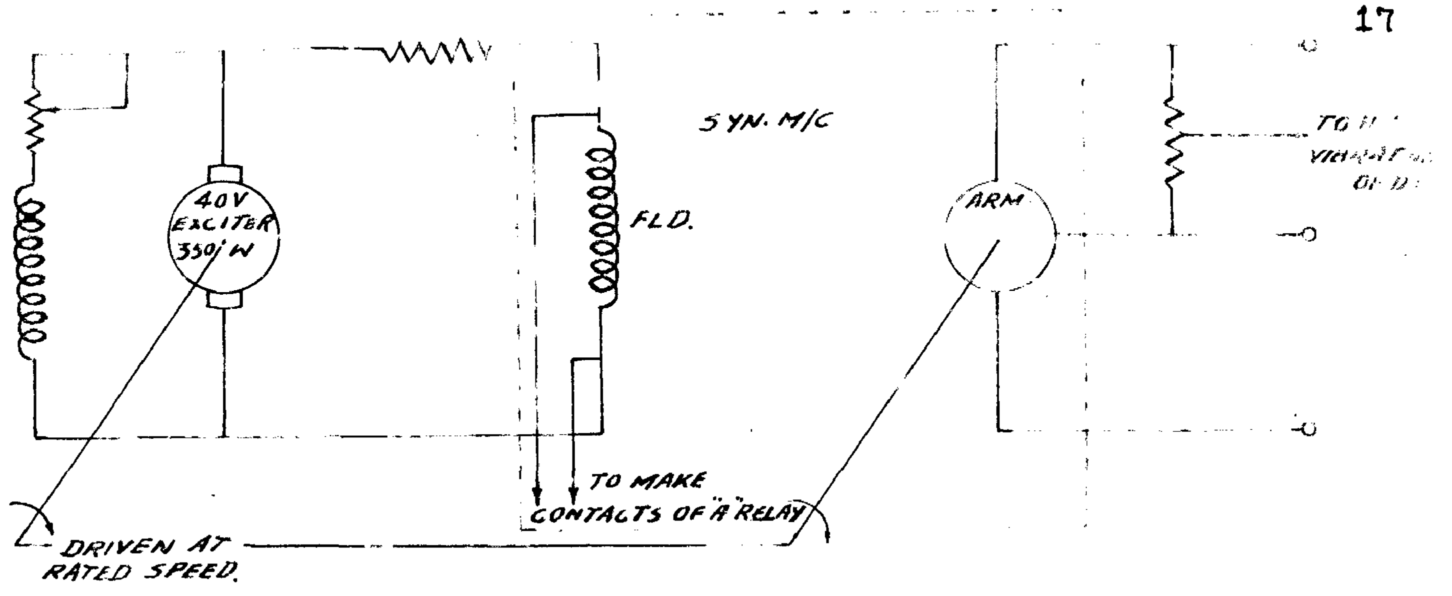

FIG.3·3 DETERMINATION OF T'_{do}.

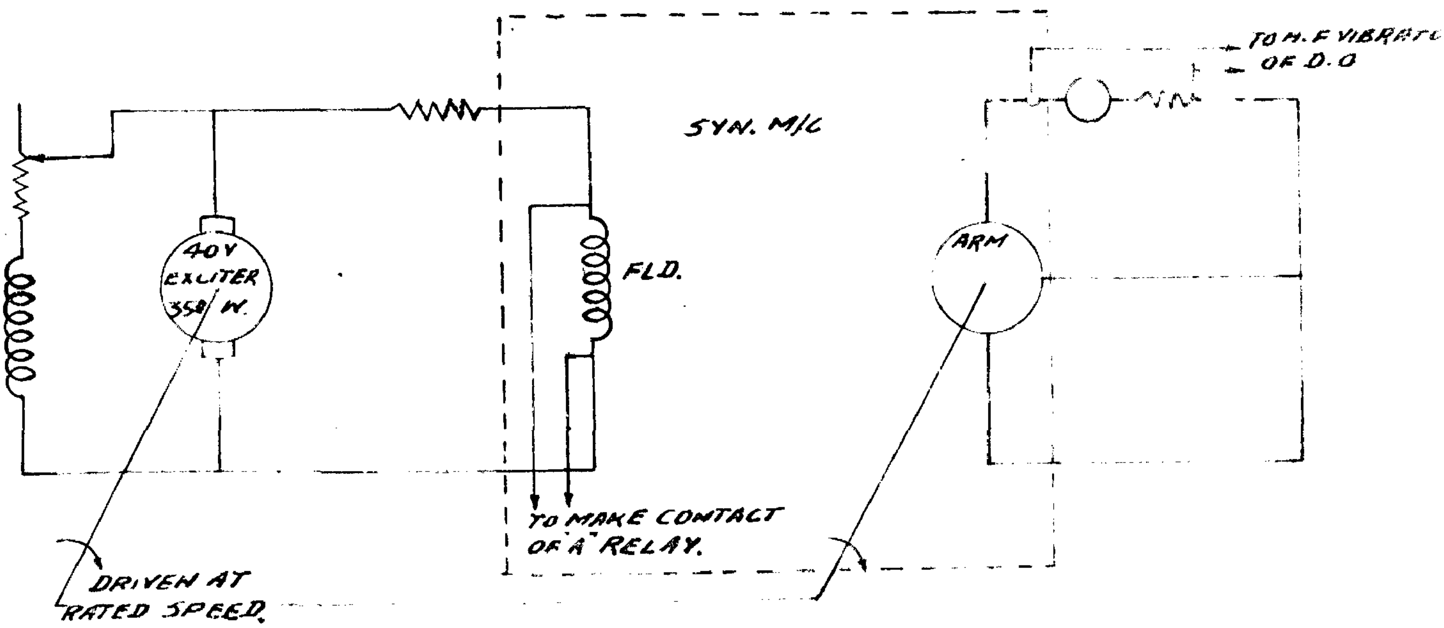

FIG.3 4. DETERMINATION OF T'_{d}

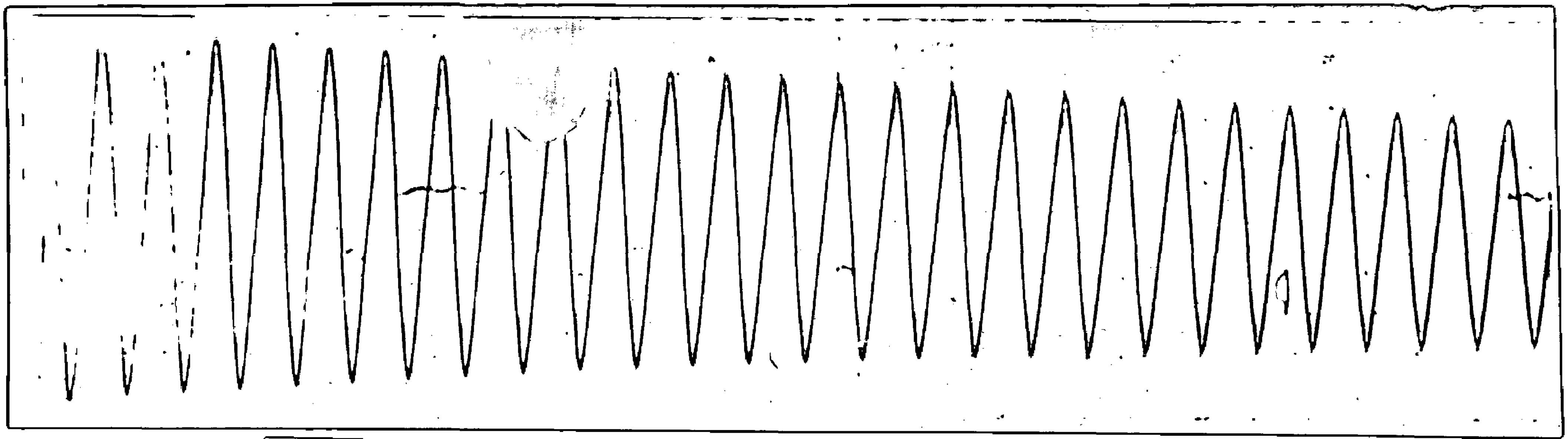

Fig.2.5. Synch. machine. Oscillogram of armature o.c. volts as field is short circuited.

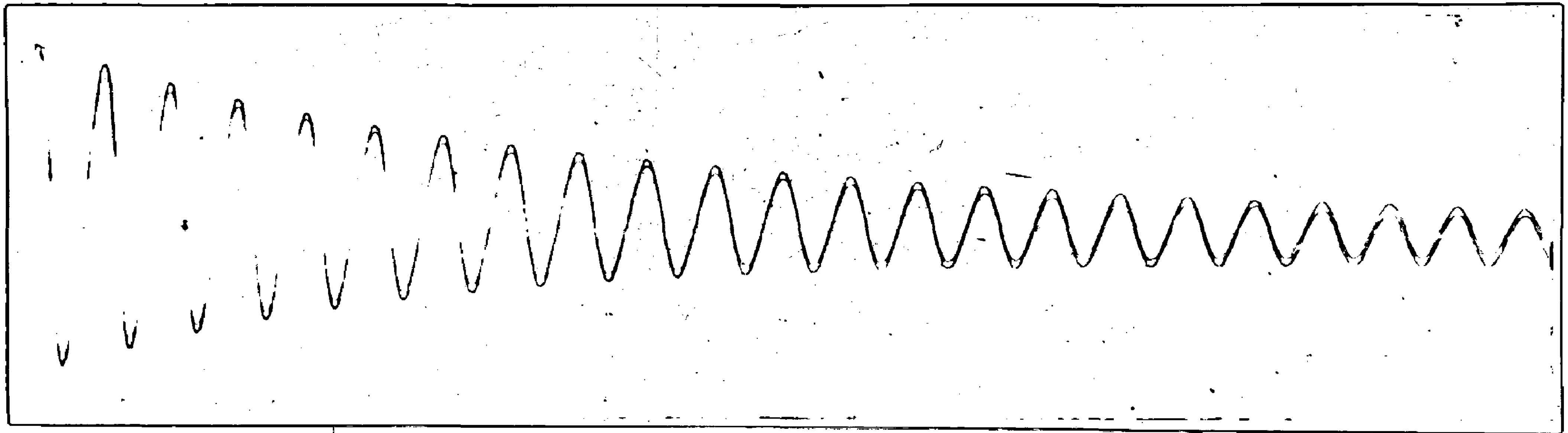

Fig.2.6. Synch. machine. Oscillogram of armature s.c. current as field is short circuited.

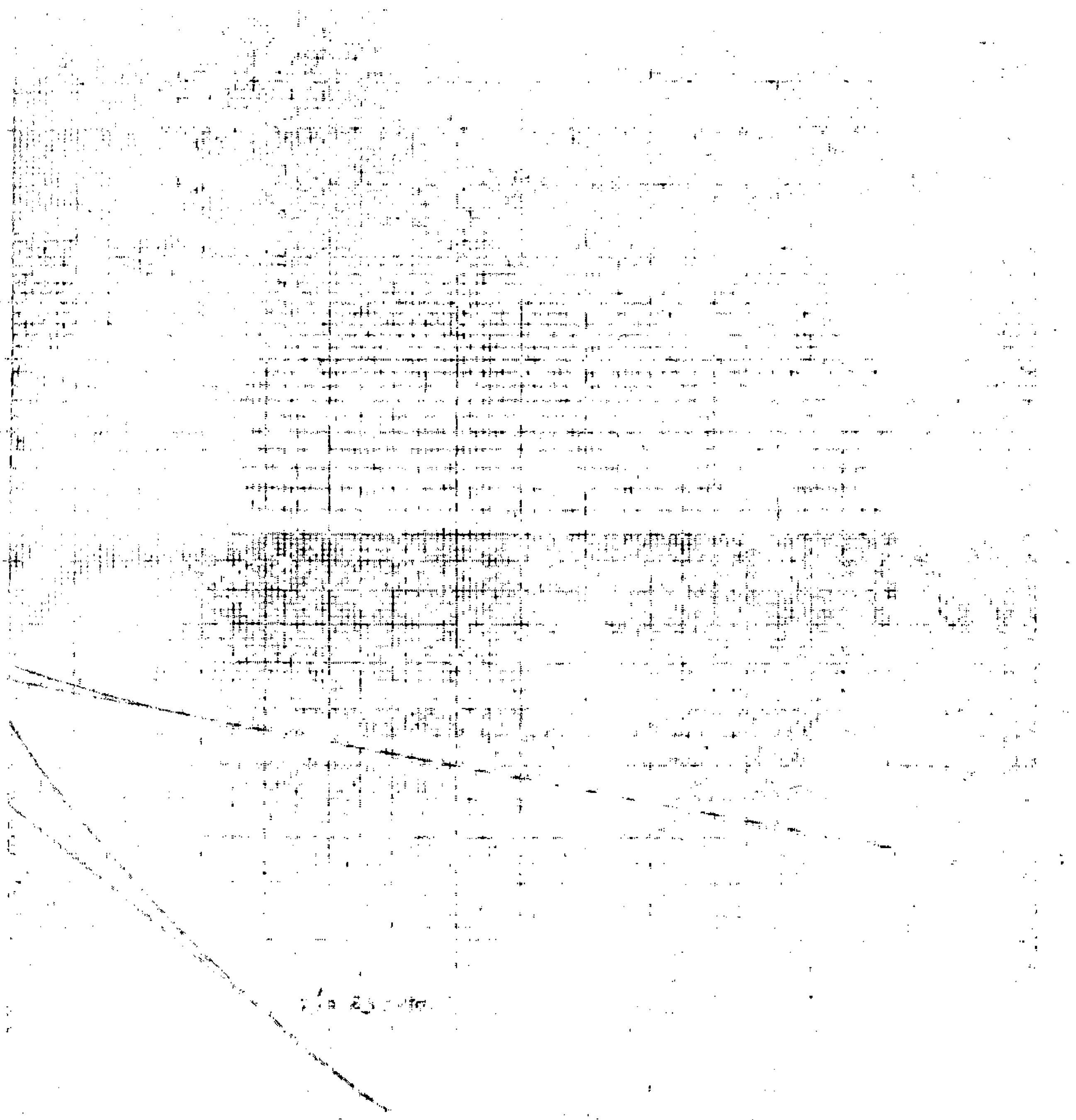

$T'_d = 0.25$ sec.

From equations (66) and (67)

$x_f = 0.1185$

$r_f = 0.00311$

3.5. MEASUREMENT OF OPERATIONAL IMPEDANCES[11] at the Synchronous frequency and hencethe determination of the damper constants;

Connections are shown in Fig.(3.8).

Input impedances, $Z_{in}\Big|_d = 2\{r + jx_d(jw)\}$ ... (68)

$Z_{in}\Big|_q = 2\{r + jx_q(jw)\}$ ... (69)

are calculated from the readings of Voltmeter, ammeter and wattmeter in the input circuit when the armature is aligned for maximum and minimum voltages respectively across the field winding. Results are,

<u>D-Axis</u>

Current = 10.8 A

Voltage = 149 V

Power = 865 W

so that $Z_{in}\Big|_d = 0.348 + j.546$

<u>Q-Axis</u>

Current = 10.8 A

Voltage = 95.5 V

Power = 590 W

so that $Z_{in}\Big|_q = 0.238 + j\ .341$

D.C. resistance test on one phase of the armature gives,

Current=10.8 A

Voltage= 11.2V

so that r = 1.035 ohm

= 0.045 P.U.

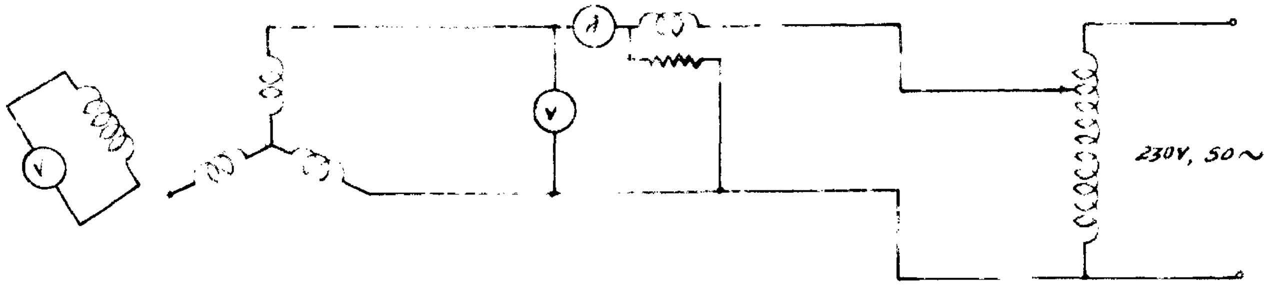

FIG. 3·8

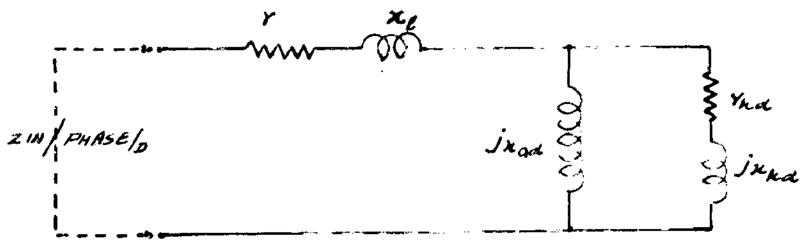

FIG. 3·9

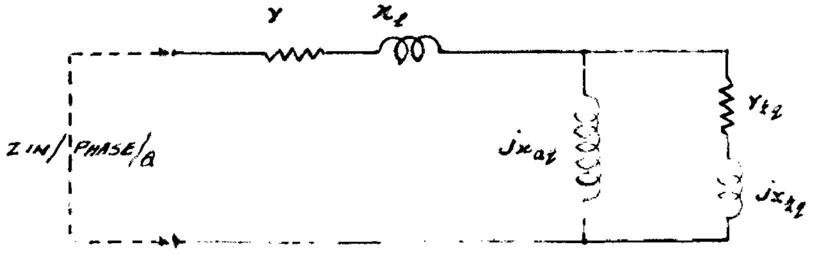

FIG. 3·10.

DETERMINATION OF OPERATIONAL IMPEDANCES.

From the equivalent circuits, Figs.(3.9), (3.10),-

$$Z_{in} \text{ per phase}\Big|_d = 0.174 + j\,0.273$$

$$r + jx_1 = 0.045 + j0.122$$

$$jx_{ad} = j\,0.958$$

so that $\underline{r_{kd} + jx_{kd} = 0.177 + j0.151}$

$$Z_{in} \text{ per phase}\Big|_q = 0.11875 + j\,0.1705$$

$$r + jx_1 = 0.045 + j\,0.122$$

$$jx_{aq} = j0.326$$

so that $\underline{r_{kq} + jx_{kq} = 0.095 + j\,0.0316}$

Summarising, the machine constants in P.U. values are:

$r = 0.045$	$x_{ad} = 0.958$	$r_{kd} = 0.177$
$x_1 = 0.122$	$x_{aq} = 0.326$	$x_{kd} = 0.151$
$x_d = 1.08$	$r_f = 0.003$	$r_{kq} = 0.095$
$x_q = 0.448$	$x_f = 0.119$	$x_{kq} = 0.0316$

CHAPTER IV

APPLICATION OF THE LARGE OSCILLATION THEORY FOR EVALUATING TORQUE NUMERICALLY IN A LABORATORY SYNCHRONOUS MACHINE

4.1. Using the constants determined in Chapter III, a numerical analysis is performed here. Assuming certain operating conditions the flux linkage coefficients are calculated; operational impedances at four oscillation frequencies 0.5, 1, 1.5 and 2 cycles per sec. in both the d and q axes are calculated; d-q axes currents are then found and torque is determined.

4.2. OPERATING CONDITIONS (P.U. SYSTEM):

$\delta_o = \frac{\pi}{6}$ elect.radians. $\qquad e = 1$

$\delta_m = .349$ elect.radians. $\qquad e_m = \sqrt{2}$

$w = 314$ elect.rad.per sec. $\qquad E_o = \sqrt{2} \times 1.2$

$f = 50$ cycles per sec. $\qquad x_d = 1.08$

$x_q = 0.448$

Using equations, 25, 26, 27, 28, 33, 34, 35, 36 flux linkage co-efficients are found to be,

$\Psi_{do} = -\sqrt{2} \times 2.675 \times 10^{-3}$ $\qquad \Psi_{qo} = \sqrt{2} \times 1.54 \times 10^{-3}$

$\Psi_{ds1} = \sqrt{2} \times 0.547 \times 10^{-3}$ $\qquad \Psi_{qs1} = \sqrt{2} \times 0.948 \times 10^{-3}$

$\Psi_{ds3} = \sqrt{2} \times 0.00637 \times 10^{-3}$ $\qquad \Psi_{qs3} = \sqrt{2} \times 0.01103 \times 10^{-3}$

$\Psi_{dc2} = -\sqrt{2} \times 0.0839 \times 10^{-3}$ $\qquad \Psi_{qc2} = \sqrt{2} \times 0.0485 \times 10^{-3}$

Fourth and higher harmonics are too ineffective to be considered.

4.3. OPERATIONAL IMPEDANCES:

$\frac{K}{2\pi} = 0.5$ cps

$x_d(jk) = 0.297 - j\,.203$ $\qquad x_q(jk) = .449 - j0.0129$

$x_d(j2k) = 0.239 - j\,.118$ $\qquad x_q(j2k) = .447 - j0.0224$

$x_d(j3k) = 0.232 - j\,.0806$ $\qquad x_q(j3k) = .444 - j0.0325$

$\frac{K}{2\pi} = 1$ cps

$x_d(jk) = .239 - j\ .118$ $\qquad$ $x_q(jk) = .448 - j\ .0224$

$x_d(j2k) = .230 - j\ .0542$ $\qquad$ $x_q(j2k) = .443 - j\ .044$

$x_d(j3k) = .219 - j\ .0379$ $\qquad$ $x_q(j3k) = .433 - j\ .064$

$\frac{K}{2\pi} = 1.5$ cps

$x_d(jk) = .232 - j\ .0806$ $\qquad$ $x_q(jk) = .444 - j\ .0325$

$x_d(j2k) = .219 - j\ .0379$ $\qquad$ $x_q(j2k) = .433 - j\ .064$

$x_d(j3k) = .207 - j .0274$ $\qquad$ $x_q(j3k) = .417 - j\ .0902$

$\frac{K}{2\pi} = 2$cps

$x_d(jk) = .230 - j0.542$ $\qquad$ $x_q(jk) = .443 - j\ .044$

$x_d(j2k) = .227 - j0.0309$ $\qquad$ $x_q(j2k) = .425 - j\ .0825$

$x_d(j3k) = .204 - j0.0216$ $\qquad$ $x_q(j3k) = .337 - j\ .112$

4.4. CURRENTS:

Equations 51, 52, 53, 54 are used-

$i_{do} = \sqrt{2} \times .36$ $\qquad$ $i_{qo} = \sqrt{2} \times 1.08$

$\frac{K}{2\pi} = 0.5$ cps

$i_{ds1} = \sqrt{2} \times .392$ $\qquad$ $i_{qs1} = \sqrt{2} \times .662$

$i_{ds2} = \sqrt{2} \times .044$ $\qquad$ $i_{qs2} = -\sqrt{2} \times .00171$

$i_{ds3} = \sqrt{2} \times .000766$ $\qquad$ $i_{qs3} = \sqrt{2} \times .00778$

$i_{dc1} = \sqrt{2} \times .268$ $\qquad$ $i_{qc1} = \sqrt{2} \times .019$

$i_{dc2} = -\sqrt{2} \times .089$ $\qquad$ $i_{qc2} = \sqrt{2} \times .0339$

$i_{dc3} = \sqrt{2} \times .00267$ $\qquad$ $i_{qc3} = \sqrt{2} \times .00057$

$\frac{K}{2\pi} = 1$ cps

$i_{ds1} = \sqrt{2} \times .578$	$i_{qs1} = \sqrt{2} \times .663$
$i_{ds2} = \sqrt{2} \times .0256$	$i_{qs2} = -\sqrt{2} \times .00339$
$i_{ds3} = \sqrt{2} \times .0088$	$i_{qs3} = \sqrt{2} \times .00785$
$i_{dc1} = \sqrt{2} \times .2885$	$i_{qc1} = \sqrt{2} \times .0332$
$i_{dc2} = -\sqrt{2} \times .1088$	$i_{qc2} = \sqrt{2} \times .0342$
$i_{dc3} = \sqrt{2} \times .001524$	$i_{qc3} = \sqrt{2} \times .00116$

$\frac{K}{2\pi} = 1.5$ cps

$i_{ds1} = \sqrt{2} \times .657$	$i_{qs1} = \sqrt{2} \times .668$
$i_{ds2} = \sqrt{2} \times .01934$	$i_{qs2} = -\sqrt{2} \times .0051$
$i_{ds3} = \sqrt{2} \times .00947$	$i_{qs3} = \sqrt{2} \times .00795$
$i_{dc1} = \sqrt{2} \times .229$	$i_{qc1} = \sqrt{2} \times .049$
$i_{dc2} = \sqrt{2} \times .1126$	$i_{qc2} = \sqrt{2} \times .0346$
$i_{dc3} = \sqrt{2} \times .00125$	$i_{qc3} = \sqrt{2} \times .00172$

$\frac{K}{2\pi} = 2$ cps

$i_{ds1} = \sqrt{2} \times .706$	$i_{qs1} = \sqrt{2} \times .665$
$i_{ds2} = \sqrt{2} \times .0154$	$i_{qs2} = -\sqrt{2} \times .0067$
$i_{ds3} = \sqrt{2} \times .00916$	$i_{qs3} = \sqrt{2} \times .0093$
$i_{dc1} = \sqrt{2} \times .1664$	$i_{qc1} = \sqrt{2} \times .0662$
$i_{dc2} = -\sqrt{2} \times .104$	$i_{qc2} = \sqrt{2} \times .0346$
$i_{dc3} = \sqrt{2} \times .00102$	$i_{qc3} = \sqrt{2} \times .00309$

4.5. TORQUE:

Even sine and odd cosine terms are absent in flux linkage coefficients, whereas, the currents possess these components also as could clearly be seen from equations 53, 54, Expanding equation 56 in the light of these remarks and neglecting harmonics of order four and higher, the equation of torque will be the summation of-

(i) Average term

$$= \frac{W}{2}\Big[(i_{do}\Psi_{qo}-i_{qo}\Psi_{do})+\tfrac{1}{2}\big\{(i_{ds1}\Psi_{qs1}+i_{dc2}\Psi_{qc2}+i_{ds3}\Psi_{qs3})-(i_{qs1}\Psi_{ds1}+i_{qc2}\Psi_{dc2}+i_{qs3}\Psi_{ds3})\big\}\Big],$$

(ii) Sin kt term

$$= \frac{W}{2}\Big[i_{do}\Psi_{qs1}+i_{ds1}\Psi_{qo}-i_{qo}\Psi_{ds1}-i_{qs1}\Psi_{do}+\tfrac{1}{2}\big\{(i_{qs1}\Psi_{dc2}+i_{qc2}\Psi_{ds1}+i_{ds3}\Psi_{qc2}+i_{dc2}\Psi_{qs3})-(i_{ds1}\Psi_{qc2}+i_{dc2}\Psi_{qs1}+i_{qs3}\Psi_{dc2}+i_{qc2}\Psi_{ds3})\big\}\Big]\sin kt,$$

(iii) Cos kt term:

$$= \frac{W}{2}\Big[i_{dc1}\Psi_{qo}-i_{qc1}\Psi_{do}+\tfrac{1}{2}\big\{(i_{ds2}\Psi_{qs1}+i_{dc1}\Psi_{qc2}+i_{dc3}\Psi_{qc2}+i_{ds2}\Psi_{qs3})-(i_{qs2}\Psi_{ds1}+i_{qc1}\Psi_{dc2}+i_{qc3}\Psi_{dc2}+i_{qs2}\Psi_{ds3})\big\}\Big]\text{Cos} kt,$$

(iv) Sin 2kt term:

$$= \frac{W}{2}\Big[i_{ds2}\Psi_{qo}-i_{qs2}\Psi_{do}+\tfrac{1}{2}\big\{(i_{dc1}\Psi_{qs1}+i_{dc1}\Psi_{qs3}+i_{qc3}\Psi_{ds1})-(i_{qc1}\Psi_{ds1}+i_{qc1}\Psi_{ds3}+i_{dc3}\Psi_{qs1})\big\}\Big]\text{Sin } 2kt,$$

(v) Cos 2kt term

$$= \frac{W}{2}\Big[(i_{do}\Psi_{qc2}+i_{dc2}\Psi_{qo}-i_{qo}\Psi_{dc2}-i_{qc2}\Psi_{do})+\tfrac{1}{2}\big\{(i_{qs1}\Psi_{ds1}+i_{ds1}\Psi_{qs3}+i_{ds3}\Psi_{qs1})-(i_{ds1}\Psi_{qs1}+i_{qs1}\Psi_{ds3}+i_{qs3}\Psi_{ds1})\big\}\Big]\text{Cos } 2\text{ kt}.$$

(vi) Sin 3 Kt term

$$= \frac{W}{2}\Big[(i_{do}\Psi_{qs3}+i_{ds3}\Psi_{qo}-i_{qo}\Psi_{ds3}-i_{qs3}\Psi_{do})+\tfrac{1}{2}\big\{(i_{ds1}\Psi_{qc2}+i_{dc2}\Psi_{qs1})-(i_{qs1}\Psi_{dc2}+i_{qc2}\Psi_{ds1})\big\}\Big]\text{ Sin } 3\text{ kt, and-}$$

(vii) Cos 3kt term:

$$= \frac{W}{2}\Big[i_{dc3}\Psi_{qo} - i_{qc3}\Psi_{do} + \tfrac{1}{2}\big\{(i_{qs2}\Psi_{ds1} + i_{dc1}\Psi_{qc2}) - (i_{ds2}\Psi_{qs1} + i_{qc1}\Psi_{dc2})\big\}\Big] \text{Cos } 3kt \quad \ldots \quad \ldots \quad ..(68)$$

Using equation 68, torque is calculated for different oscillation frequencies. Table I below summarises the torque-variation as the frequency is changed.

Table I

$\frac{K}{2\pi}$	Amplitude of Torque terms						
	Average	Sin kt	Cos kt	Sin2kt	Cos2kt	Sin 3kt	Cos 3kt
0.5	1.083	.672	.155	.0582	.0183	.00494	-.00262
1.0	1.11	.765	.173	.0495	-.0179	.00399	.00198
1.5	1.12	.805	.158	.0356	-.0311	.00438	.001125
2.0	1.13	.827	.138	.0211	-.0341	.00707	.00236

CHAPTER V

AN EXPERIMENTAL SET UP FOR INVESTIGATING THE LARGE OSCILLATION THEORY

Block diagram in Fig.(5.1) describes the set up. The synchronous machine referred to in Chapter III is driven by its d.c. motor. A magnetic coupled torque meter is interposed between the driving d.c. motor and the driven synchronous machine for recording the torque variations. The signal from the torque meter, a voltage, is recorded on a C.R.O. An a.c. tachogenerator is coupled to the machine shaft at one of its free ends to provide a voltage signal in phase with the shaft position relative to a synchronously revolving field. A phase shifter worked off the bus bars which produce the synchronously revolving field provides the reference voltage signal. Both the signals are clipped, converted into square waves, differentiated and amplified to give sharp pulses which modulate the beam intensity of a C.R.O. and appear as spots on the x-axis when its time base is synchronised with the line frequency. A camera with its film moving in the y-axis at a constant speed records these spots giving the load angle variation as a distance between the reference zero spot (due to the bus bar signal) and the moving spot (due to the tacho-generator signal).

A 12 inch diameter x ¼ inch thick bakelite disc with 90-0-90 degree graduations on its half circumference is fixed to the machine shaft so that by making stroboscopic observations the machine can be set to oscillate with known amplitude. A precision wattmeter is connected to measure the power transfer between the synchronous machine and the bus. When this meter reads zero indicating thereby that the machine is on no load, the shaft angle is zero. The disc is clamped to the shaft in such a position that its zero graduation coincides with the stationary cursor arrangement

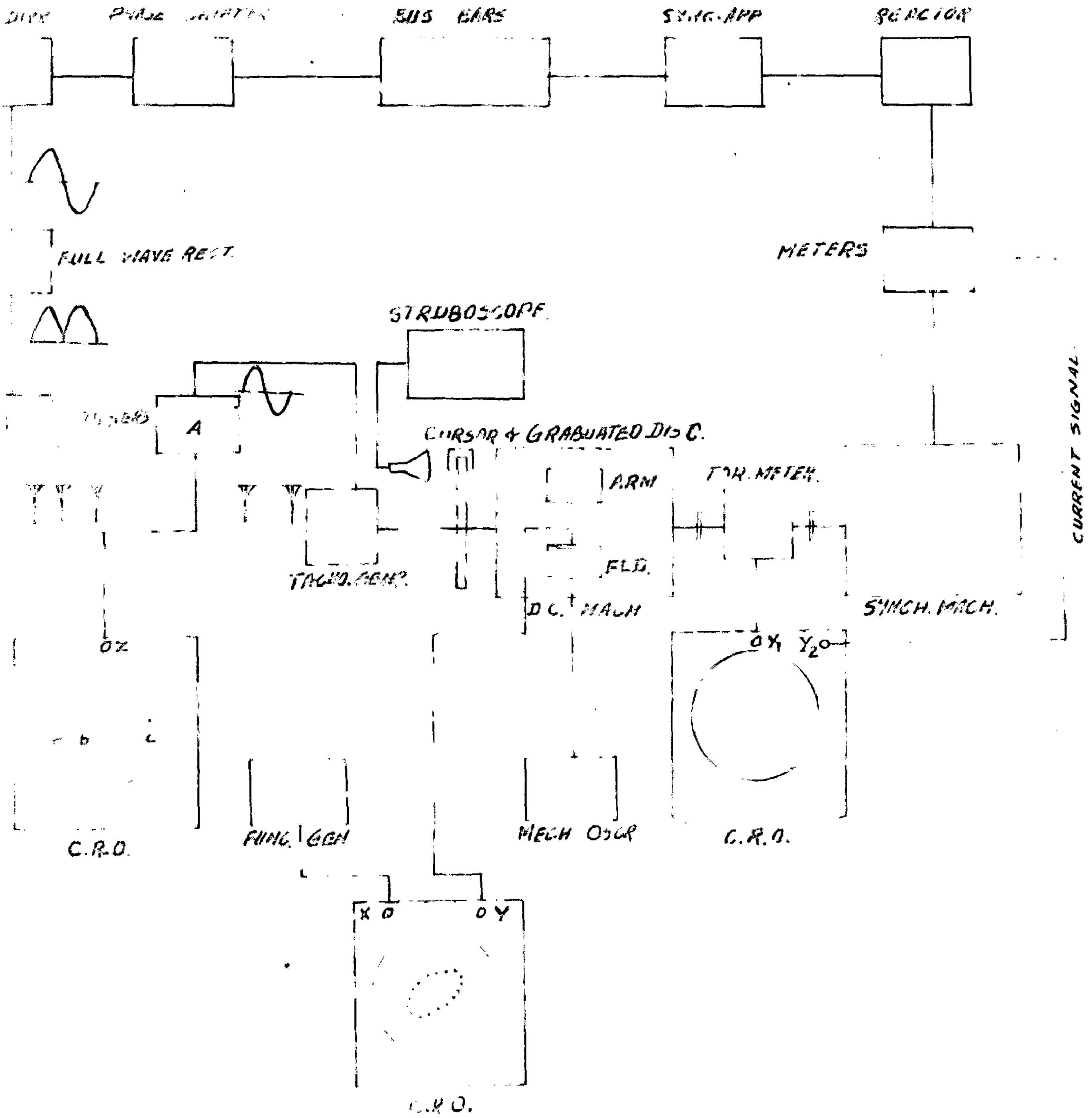

BLOCK DIAGRAM OF THE EXPERIMENTAL SET-UP when the machine is on no load. Load angle can now be read strobo-scopically quite precisely.

A resistance in the field circuit of the driving d.c. motor is mechanically varied sinusoidally to produce a sinusoidal oscillation in the field current, torque and hence in the load angle. Oscillation frequencies from 0.5 cps to 2 cps are produced by controlling the speed of the d.c. motor which drives the rheostat brush through an eccentric rod on a circular driving plate. These frequencies are checked by forming Lissajous pattern on a D.C. Oscilloscope using a low frequency function generator as reference.

A 3 phase reactor is inserted between the synchronous machine and the bus bars. This will help (1) to limit the current and (2) to obtain a greater divergence in the load angle without over current and instability. While studying the transient behaviour of the synchronous machine, the reactor will also help in creating transients at will by suddenly inserting it into or deleting it from the circuit partially or wholly.

The torque and load angle recording devices and the low frequency oscillation generating device are described and discussed in later chapters.

CHAPTER VI

DESIGN, FABRICATION AND CALIBRATION OF A TORQUE RECORDING DEVICE: SURVEY OF EARLIER WORK

6.1. Numerous methods have been developed from time to time for measuring the torque transmitted by a driving member to a driven member. Whereas it would be quite unnecessary to discuss the purely mechanical ones developed before 1910, it would be worth the while to touch briefly upon the more sensitive and accurate ones developed later than 1940.

Carter and Shannon[12,13] deviced capacitive strain gauges based on the principle that the capacity of a condenser arrangement fixed on a certain length of shaft varies linearly with the angle of torsional twist of that length of shaft and that a measure therefore of the change in capacity is a measure of the torque transmitted since-

$$\frac{T}{I_p} = \frac{G\theta}{l}$$

where T is the torque transmitted along a length l of shaft of polar moment of inertia I_p. θ is the angle of twist and G is the modulus of rigidity of the shaft material. Since capacity C is give by-

$$C = \frac{KA}{4\pi d},$$

with K, the dielectric constant of the medium,

A, the area of conductor plates, and

d, the separation distance between the conducting plates, it is usual practice to keep K constant and use A or d to transduce the torque. The former is better since it permits unlimited mechanical movement while the latter has the limitation that the physical contact of the condenser plates results in short circuit.

Developed later are the resistance strain gauges[14,15] based on the principle that their resistance changes linearly with the tension or compression induced along the principal planes of the shaft subjected to torsion. A single bonded wire gauge placed such that it follows a 45^o helix on the shaft surface would experience maximum strain due to thetorque and would conveniently measure the torque. But any bending or thrust applied to the shaft would affect the gauge response and any change in temperature would give false gauge readings. Sliprings and brushes are necessary for connection to the external measuring circuit. The variable brush contact resistance can become comparable unless the gauge resistance is quite high.

Some of the above said limitations of a single bonded wire gauge can be overcome by arranging four gauges as in Fig.(6.1) forming a wheatstone bridge. Its opposite arms will be gauges subjected to the strains of the same sign. The bridge gets unbalanced due to the torque and is not affected by bending and thrust.

A thrust along the shaft axis will cause equal changes in all the four arms and the balance of the bridge is thus not affected. A bending moment acting about a vertical axis of the section makes A and B suffer strains equal and opposite to those suffered by C and D and thus the balance is yet undisturbed. Similarly a bending moment about a horizontal axis would leave the balance unaffected since the net change in each arm would be zero. This is an important advantage not possessed by the other types of torque meters without elaborate precautions. The meter is temperature-compensated too because of the proximity of the gauges. Since the gauges rotate with the shaft, sliprings and brushes are needed for connection to the external measuring circuit. For their suitability they must have low contact

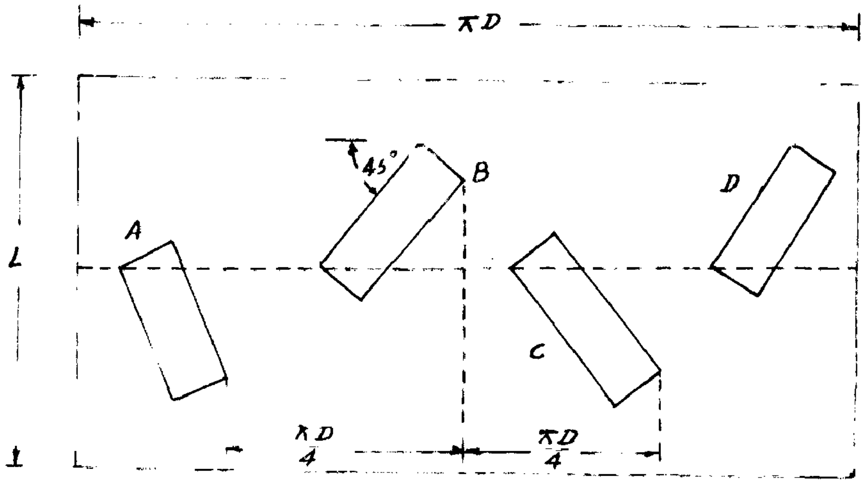

ARRANGEMENT OF THE STRAIN GAUGES.

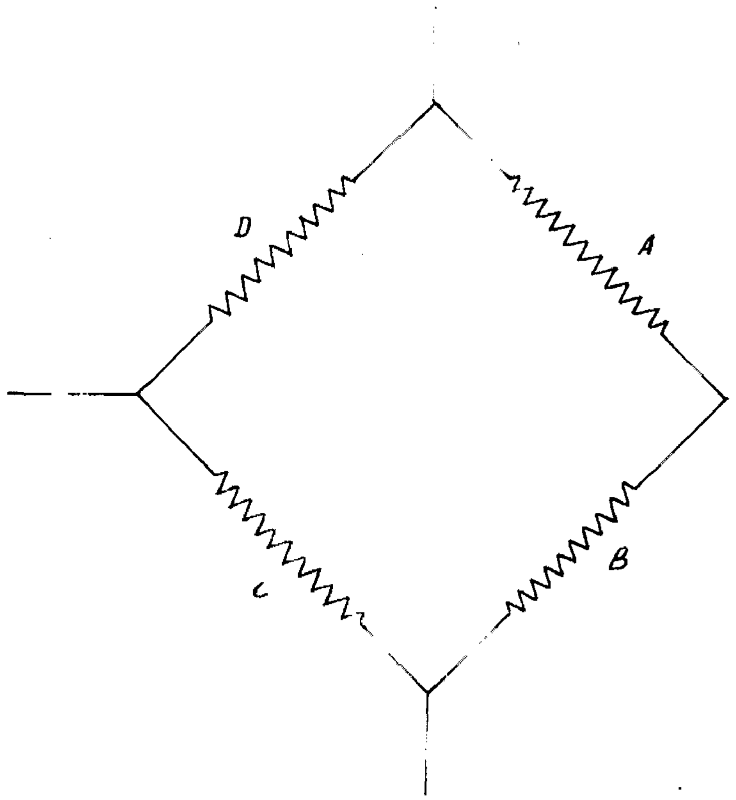

FIG 6.1 STRAIN GAUGES CONNECTED IN A BRIDGE

potential and resistance which must remain constant over a wide range of rubbing speeds. The noise they generate should be negligible since a high gain amplifier will generally be required, the output signal being weak. Silver sliprings because of the high electrical conductivity and carbon brushes because of their good lubricational properties form the best combination.

A standard circuit for recording transient or dynamic torques is shown in fig.(6.2)

The meter accuracy depends upon the magnitude of the shaft strain. Higher working stresses are therefore desirable. Alloy steels are ideal materials for the pick-up shafts. A serious limitation is the relatively large temperature coefficient of resistance of the resistance strain gauges.

Literature[16] describes a torque meter using micro waves in a cavity resonator. Cavity is a space enclosed by walls of high electrical conductivity in which high frequency electromagnetic waves are excited. The points at which resonance occurs are a function of the cavity dimensions. If power at fixed frequency is fed into the cavity, the output power transferred through the cavity (which can be measured by using a crystal detector) varies with the cavity length when it is cylindrical. The relationship between the power transferred through the cavity and the displacement is shown in Fig.(6.3).

Torque meters based on the change of permeability of certain ferromagnetic materials as the shaft twists under torque dispense with the use of slip rings and brushes resulting in the elimination of errors associated with them. This change in permeability produces a change in the inductance of, and hence a change in the

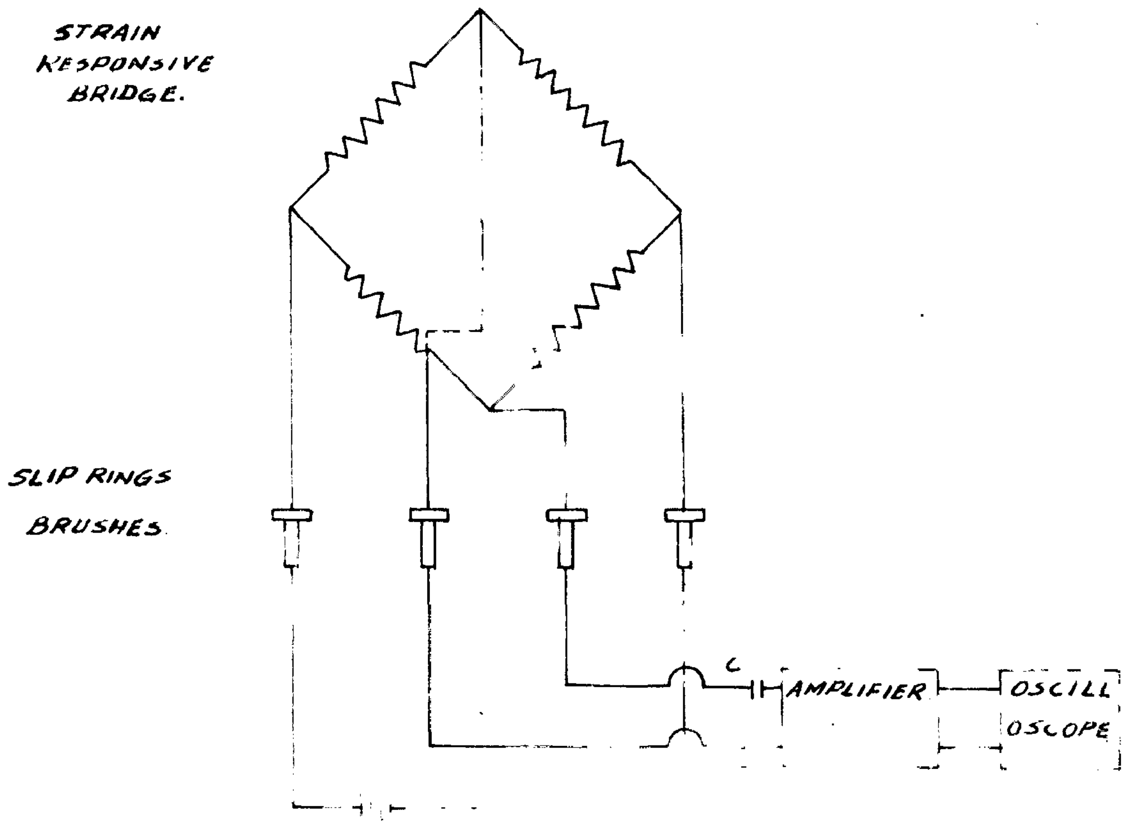

FIG. 6.2 DETERMINATION OF DYNAMIC TORQUE.

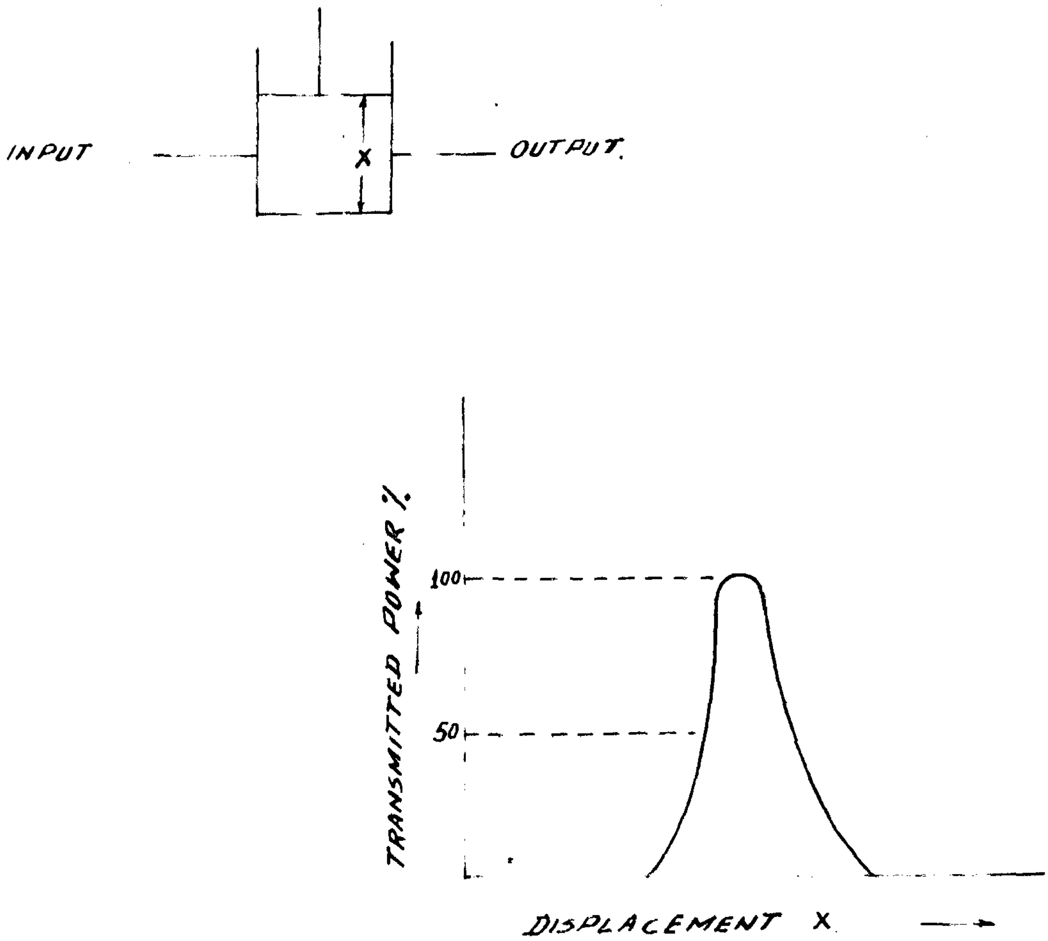

FIG. 6.3 CAVITY RESONATOR.

current in a coil wound on the shaft and fed from an a.c. source. The torque transmitted is therefore transduced into a current signal which can be amplified and recorded. These meters require a high frequency power source and they are sensitive to temperature changes, shaft bending and thrust loads, and hysteresis.

Langer[17] developed the magnetic coupled torque meter, an isometric view of which is shown in Fig.(6.4). A steel shaft has three flanges over which are mounted three toothed rings of magnetic material using non magnetic brass spacers to prevent contact with the shaft. Two sets of active air gaps are arranged, one between the outer ring 2 and the middle ring 1 and the other between the outer ring no.3 and the middle ring 1. As the shaft transmits torque one set of gaps shortens and the other lengthens. The shaft assembly is surrounded by two stationary coils one of which is excited from an a.c. source. A signal is produced in the other which varies with the torque transmitted.

The torque recording device used here is a design based on this principle.

6.2. DESIGN OF THE TORQUE METER:

A hollow shaft is chosen since the angle of twist is more for it than for a solid shaft for the same torque transmitted. This could be seen from the equations,

$$\theta = \frac{Tl}{GI_P} \text{ and } I_P = \frac{\pi}{32}(D_2^4 - D_1^4)$$

where D_1 and D_2 are the inner and outer diameters of the hollow shaft and the others have meanings already touched. To increase θ and hence the sensitivity of the meter

(i) G should be as small as possible,

(ii) I_P as small as possible and

(iii) the gauge length as large as possible.

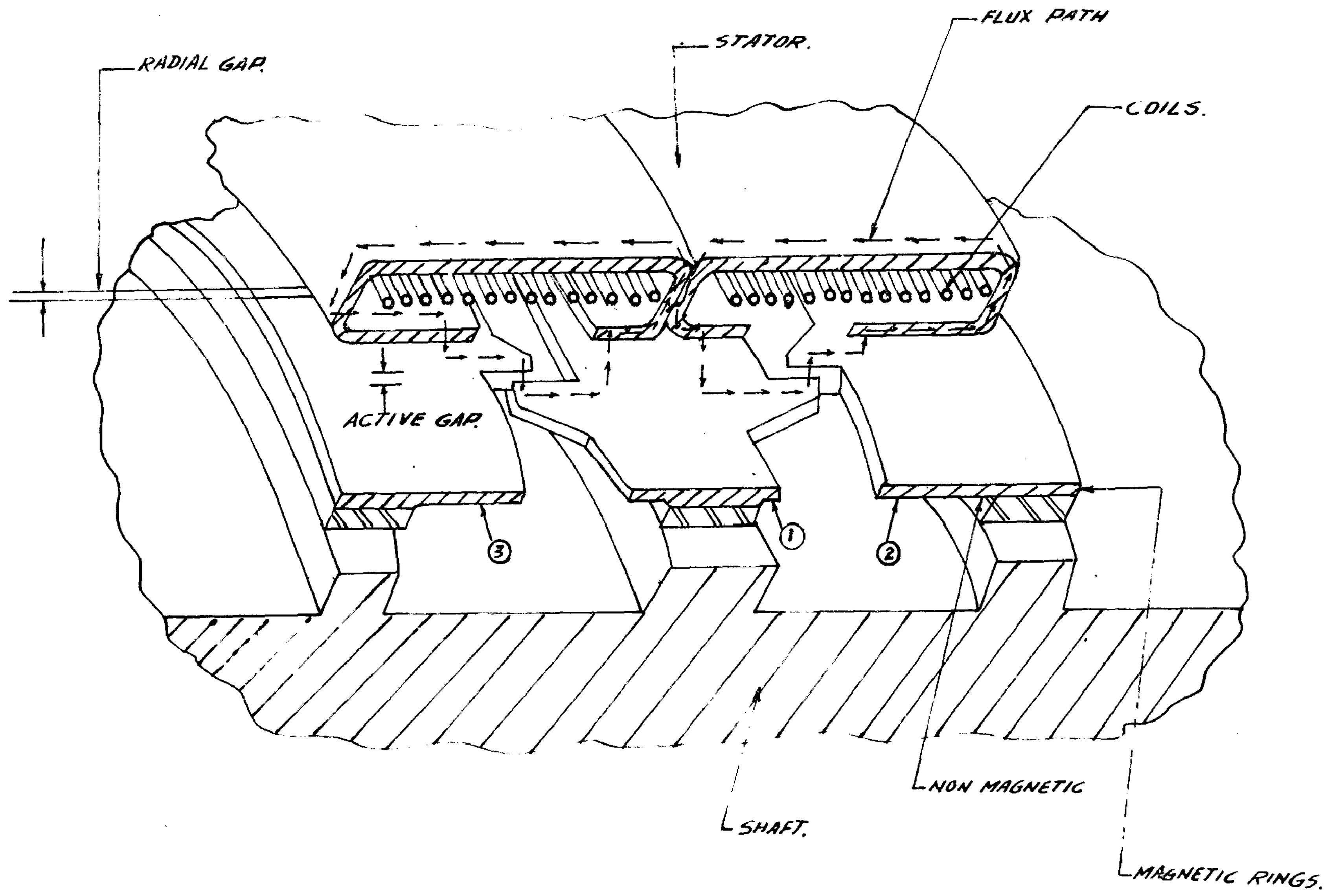

FIG. 6.4. ISOMETRIC VIEW OF MAGNETIC COUPLED TORQUE METER.

Mild steel is suitable because of its high yield point stress and good strainability. As the torque meter, interposed between the driving and driven members, should not affect the performance of the machine under test, it must have low inertia and large stiffness. The shaft and the couplings are made as light as possible. High stiffness requires a shorter length of shaft while the same minimises sensitivity by reducing θ. A compromise is therefore made.

Shaft: In the present case the shaft is designed for transmitting 10 h.p. at 1500 r.p.m. so that-

$$T = \frac{33000 \times 10}{2\pi \times 1500} = 35 \text{ lbs.ft.}$$

Fig.(6.5) is a drawing of the shaft used in the present work. Figs.(6.6) & (6.7) show the spacer rings, toothed ring and pulleys. Twist should be within limits so that the shaft may not fail in shear at the greatest vulnerable sections, namely a and b. Now,

$$I_p = \frac{\pi}{32}\left\{ \left(\frac{1}{8}\right)^4 - \left(\frac{3}{4}\right)^4 \right\} = 0.0266 \text{ in.}^4$$

and f_s, the maximum shear stress

$$= \frac{T}{I_p} \times \frac{D_1}{2}$$

$$= \frac{35 \times 12 \times 7}{0.0266 \times 16}$$

$$= 6900 \text{ psi.}$$

which is well within 10000 psi, the permissible maximum shear stress with a factor of safety, 2. Thus an inner diameter of $\frac{3}{4}$" and an external diameter of $\frac{7}{8}$" at the sections a and b are suitable. Other diamensions such as, collars for bearings and rings, key ways etc. are fixed just from a convenience point of view. The length of the test sections a and b is decided from the shaft twist required to produce a change of 10% to 20% in the active gap lengths so that the variation lies in the linear region.

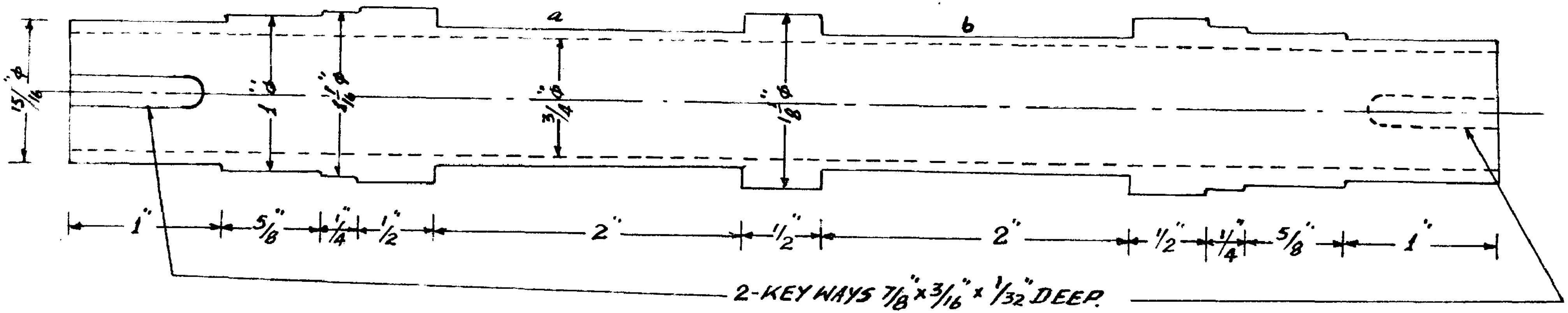

FIG. 6.5 MILD STEEL SHAFT.

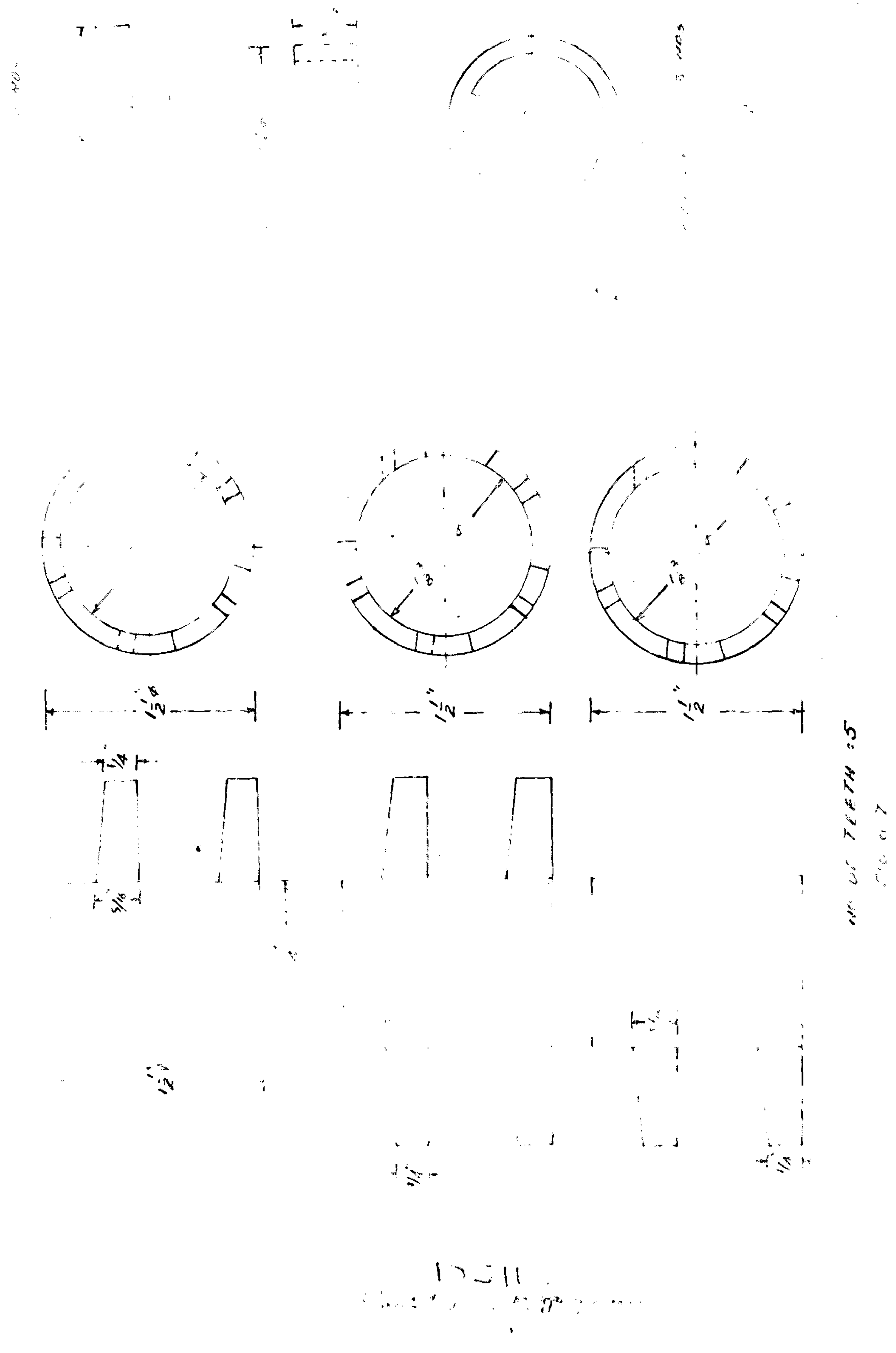

Non magnetic spacers can not be too thin to permit flux leakage into the shaft not can they be too thick to reduce the twist contributed by the collar parts of the shaft. They are chosen to be $\frac{1}{8}''$ thick. The magnetic toothed rings are chosen to have a thickness of $\frac{1}{8}''$. This would make the outer diameter at the collars to a total of $1\frac{5}{8}''$.

Now I_p, collar sections $= \frac{\pi}{32} \left[(1\frac{5}{8})^4 - (\frac{3}{4})^4 \right] = 0.655$ in^4.

I_p, test sections $= \frac{\pi}{32} \left[(\frac{7}{8})^4 - (\frac{3}{4})^4 \right] = 0.2666$ in.^{4}

Assuming G to be the same for mild steel and brass total twist θ will be the sum of the twists of the three collars and two test sections. Thus,

$$\theta = \frac{35 \times 12}{12 \times 10^6} \left[\frac{3 \times .5}{0.655} + \frac{2 \times 2}{0.0266} \right] \text{ radians.}$$

$$= 0.305^\circ$$

Twist in half gauge length $= 0.153^\circ$

The active gap length is kept at 10 mils; the criterion is that it be as small as possible limited by considerations of physical contact of the teeth under the extreme loading conditions.

The twist of 0.153° corresponds to a change in active gap length,

$$= \frac{\pi \times 1\frac{1}{2}}{360^\circ} \times 0.153^\circ, \quad (1\tfrac{1}{2}'' \text{ is the mean diameter of the ring}$$

$$= 0.002''.$$

Therefore change in active gap length as a percentage of original gap $= \frac{0.002}{0.01} \times 100$

$$= 20\%$$

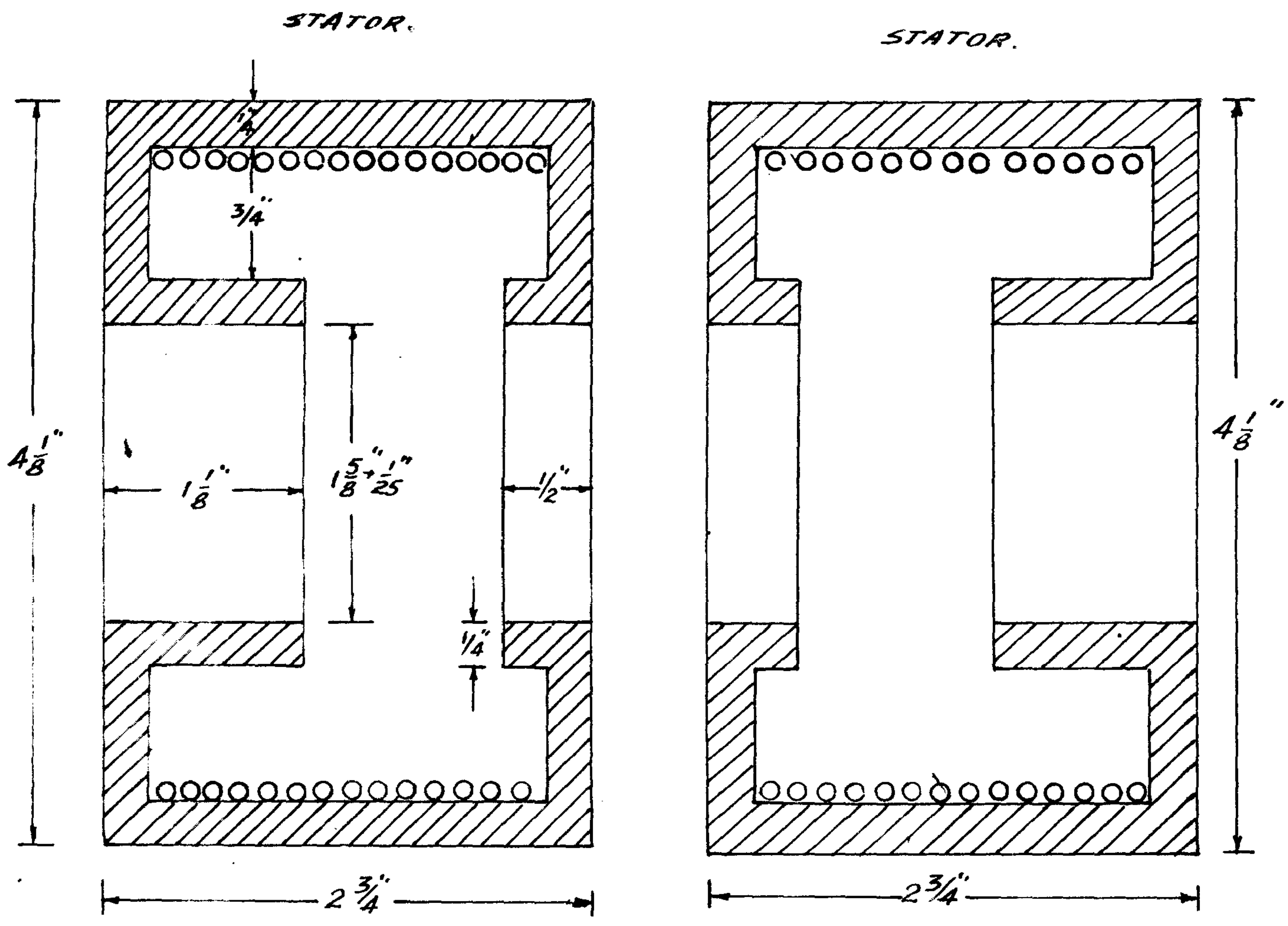

FIG. 6.8. STATOR FOR MAGNETICALLY COUPLED TORQUE METER.

Toothed Ring:

Number of teeth is chosen as 5 rather than 10 or 15 so that with smaller number of teeth magnetic leakage around the rotor is less and the sensitivity is more. The rings on assembly do not touch each other axially and are separated considerably so that separation is large enough to force the flux through the active gaps.

Stator:

The drawing in Fig.(6.8) shows the stator which consists of two equal sections along the longitudinal axis covering the shaft assembly. Stator to rotor radial gap which has negligible effect on the performance of the torque meter is set at 0.25". The stator housings are deep enough to accommodate 2 coils of 585 turns each. One set of two coils is excited in series while the other set connected in series opposition provides a signal which varies with the torque transmitted and can be recorded on a C.R.O. Output torque of the driving motor can be calculated from the readings of its input meters and a calibration curve can be prepared.

CHAPTER VII

DESIGN AND CONSTRUCTION OF A LOAD-ANGLE RECORDING DEVICE; SURVEY OF EARLIER WORK

7.1. Load angle of a synchronous machine connected to infinite bus is the time phase angle difference between the excitation voltage of the machine and the voltage of the infinite bus. It is also the angle of physical displacement of the rotor with reference to a synchronously revolving axis. (This is true under transient conditions also).

To measure the load angle, therefore, it is only necessary to obtain an electric signal proportional to the rotor angular position and compare its phase with another reference electric signal. The latter is conveniently obtained from the bus bars (or the machine terminals if no external reactor is connected in between). If the load angle relative to a particular point in a power system is required, it is only necessary to obtain the reference signal from that point. This, perhaps, may necessitate the running of special wires for this purpose; but the communication lines running below the power lines may be used with advantage!

A 'Rotor position pick-up' may be any one of the following:

(i) Tachogenerator,

(ii) Magnetic pick-up,

(iii) Photo pick-up

(iv) Shaft-operated synchronous switch.

A tachogenerator coupled directly to the rotor shaft generates a single phase a.c. signal whose phase follows the rotor position with respect to a synchronously rotating reference axis. A disadvantage of the tachogenerator is that its output may contain large harmonics that may be misinterpreted by the switching circuits. Another disadvantage, but less serious, is that the number of poles on it may be different from that on the machine. In such a case frequency multipliers become necessary.

A magnetic pick-up consists of a coil suitably located around the shaft. When a screw or a key on the shaft moves in and out of the coil magnetic circuit, its reluctance will change and a pulse is generated whose phase will follow the rotor position. This method may have a time delay owing to the inductive circuits.

A photo pick-up produces a pulse corresponding to the rotor position when it receives interrupted light from a source through a hole in an opaque disc mounted on the shaft. This has the smallest time delay and also simple in arrangement.

A shaft operated synchronous switch[18] is a mechanical contactor having all the troubles associated with a mechanical switch. Contact resistance varies with contact pressure, the speed of the rotating member, the surface conditions of the rotating member and wear of the rubbing contacts and atmospheric conditions.

7.2. SURVEY OF EARLIER WORK:

A host of methods has been available for the measurement of load angle.

A stroboscope has been successfully used by several authors to make both a qualitative study and a quantitative measurement. Powell[19] obtains a pictorial record of the rotor movement on a cine camera using a stroboscope to illuminate a mark on the rotor. These cine recording troubles were completely eliminated by Holloway[20] who used a C.R.O. type Camera. Fig.(7.1) describes his setup. He introduced reference markers at equal angular intervals, using pinholes with lamps behind. A switching time marker too was added by providing a mechanical contactor extension.

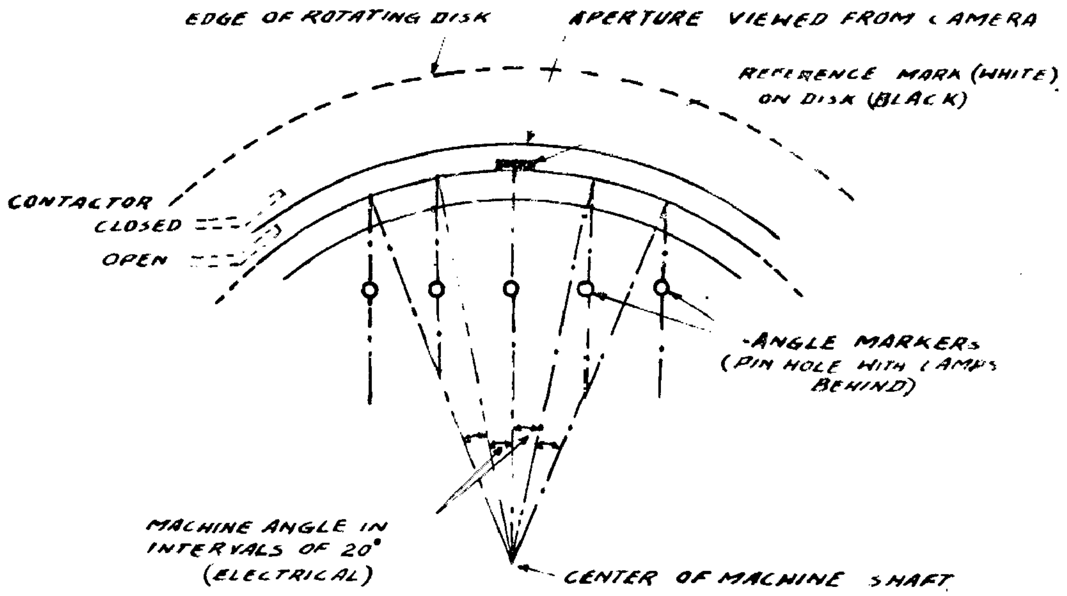

VIEW FROM CAMERA LENS.

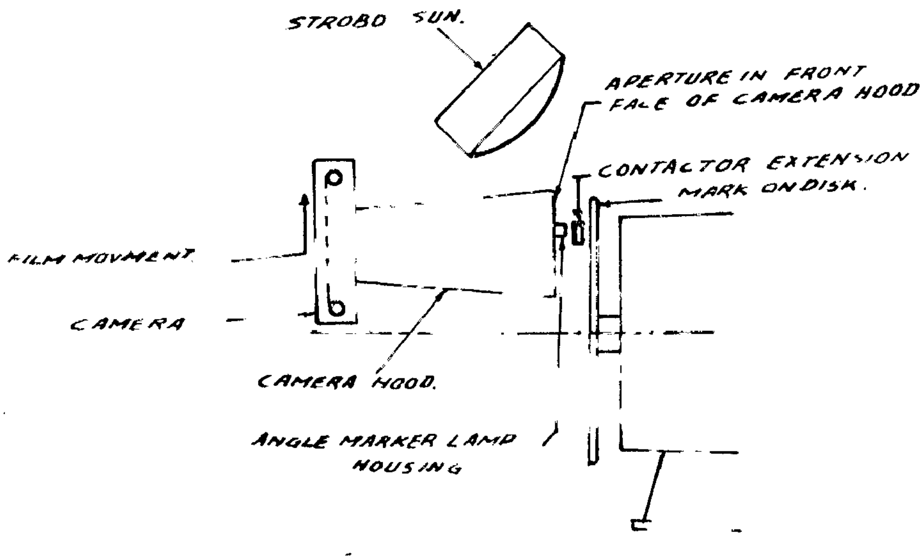

FIG. 71 VIEW SHOWING EQUIPMENT LOCATION

Film speed, it is claimed, need not necessarily remain constant. Reason for this lattitude is that the time interval is defined by the triggering pulses of the stroboscope. This would therefore necessitate that the stroboscope be of good quality and possess stability. An accuracy of $\pm 1^{\circ}$ is claimed.

A disadvantage with these methods is that one has to wait for the results till the films are developed. A pen recorder with high response speed overcomes this drawback. Prewett[21] describes in his paper the use of a high speed pen recorder driven by the d.c. component of the phase detector output. All these methods are suitable for transient recording also; but they are complex and elaborate in arrangement.

Charlton[22] used switching transistors for load angle measurements. Fig.(7.2) describes the circuit connections. Transistors T_1 and T_2 conduct during the positive and negative half cycles alternately of the terminal voltage while T_3 conducts only for half cycle of the voltage of a tachogenerator coupled to the shaft. The average voltage across AB is proportional to the load angle and is read by a centre zero moving coil instrument. The meter reading is a linear function of δ . A stabilised d.c. supply for the transistor is essential and a drift in T_3 due to temperature changes would alter the meter readings. The method is suited for steady state measurements.

A magslip[23] can be used to measure the phase difference between the busbar voltage and the tachogenerator voltage.

Another conventional method[24] is to convert both tachogenerator and bus bar signals into square waves by clippers and add them using a cathode follower. The average output of the cathode follower would be proportional to the load angle.

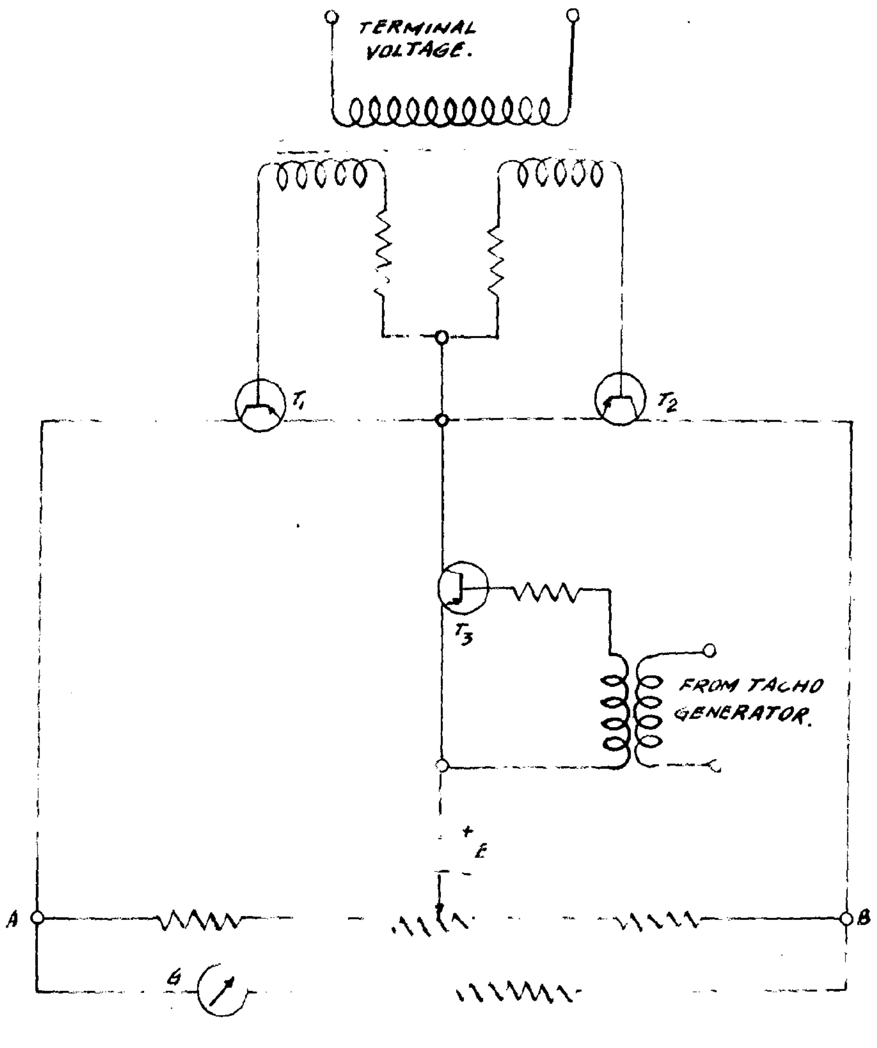

FIG 7·2 PHASE DETECTOR.

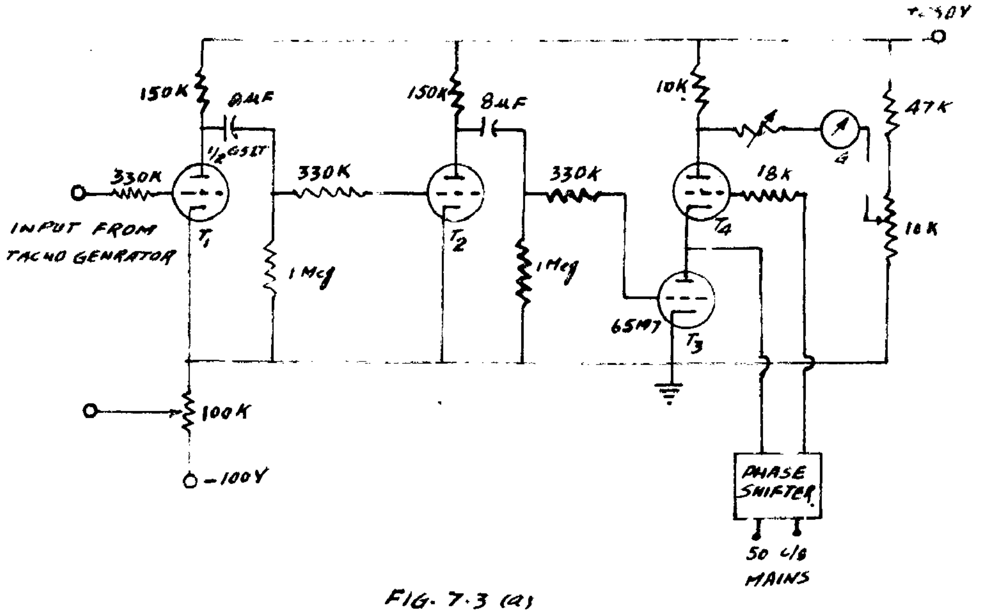

FIG. 7·3 (a)

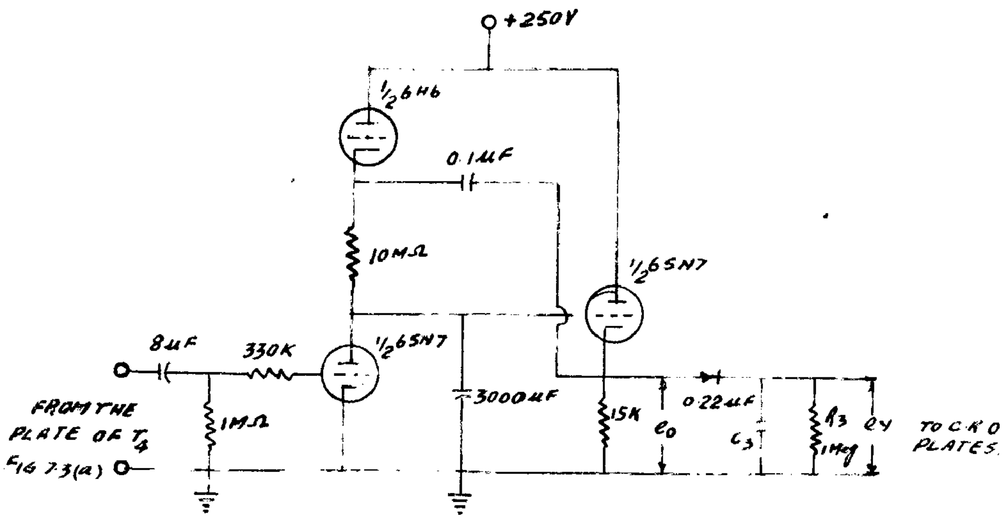

FIG. 7·3 (b)

Literature[18] describes a novel method possessing a unique feature that the signal from the tachogenerator need no longer be of the same frequency as the reference signal from the bus bars. Referring to Fig.(7.3 a) triodes T_1 and T_2 convert the tachogenerator signal into square wave during whose positive half cycle only the triode T_3 can conduct. To the grid of the thyratron T_4 bus bar voltage is applied through a phase shifter by the help of which T_4 is adjusted to conduct as long as T_3 conducts. A moving coil meter connected as shown should give a minimum reading and can be used to measure steady state angles. For transient measurements, the output of T_4, which is in the form of a train of pulses with their widths proportional to the load angle is fed to a bootstrap sawtooth generator, fig.(7.3b), whose output is in the form of a train of sawtooth waves with their amplitudes proportional to the instantaneous load angle. This can be displayed on a C.R.O. and photographed.

A paper by Kinitsky[25] describes the successful application of an electro dynamometer Wattmeter for measuring the load angle under steady state conditions. A two element dynamometer wattmeter, stripped of its control spring, gives a deflection proportional to the ratio of a.c. power flow in the lines (energising the upper element) to the steady state stability limit (energising the lower element) and hence measures sine of the load angle.

Literature[26] describes the use of a three phase, three element induction type energy meter for making load angle measurements in the steady state.

These methods suited for steady state conditions only have a good degree of accuracy. Besides, they possess an excellent advantage that there are no mechanical fixtures, such as, tachogenerator, mechanical contactor, etc., on the rotor shaft. The meters, therefore, are readily applica ble to any machine having any number of poles.

Sudan[5] in 1960 developed a new method for transient recording of load angle. Pulses from a magnetic pick up after sharpening through a differentiating circuit were used for modulating the intensity of a C.R.O. beam while a saw tooth or a sinusoidal voltage derived from the bus bars was applied to the Y plates with the internal time base synchronised to display suitable number of cycles. If the Y plates were continuously energised a saw tooth or a sine wave would appear on the screen, but as a result of Z modulation (intensity modulation is also known as Z modulation) by the pulses a series of spots spaced at intervals of one cycle would appear. The vertical displacement of the spot is proportional to the load angle or its sine depending upon whether a sawtooth wave or a sine wave is applied to the Y plates. Transient oscillation of the load angle is indicated by the variation in the vertical position of the spots from the x-axis. A phase shifter is used to set the initial displacement of the spot to zero when the machine is on no load.

The load angle recording device developed and used here is based on this method with certain modifications.

7.3. MODIFIED LOAD ANGLE RECORDING DEVICE:

Certain modifications are introduced resulting in a simple system. The transistor pulsing circuits developed here are extremely simple and replace the complex and elaborate electronic circuitry of earlier works. The method can be applied to any machine readily. Particularly, if the tachogenerator is replaced by a photoelectric pick-up for producing the shaft signal, the method becomes more versatile in the sense that the frequency multipliers would no longer be necessary which are otherwise needed if the tachogenerator had a different number of poles than the synchronous machine.

Referring to Fig.(5.1), the block diagram of the experimental set up given in Chapter V, pulsor A (details in Fig.7.4a) produces pulses at the instants the sinusoidal shaft signal passes through zero. The output of the emitter follower consists of two pulses 360° apart, i.e. a cycle apart, the one at 180° being eliminated by it. Even otherwise this pulse is ineffective during Z-modulation it being a positive pulse; but an emitter follower is necessary to raise the power level of these pulses. Pulser **B** receives the reference signal at its input terminals from the bus bars through a phase shifter, a potential divider and a full wave bridge rectifier. Since the polarity of all the three pulses at the voltage zero is the same the emitter-follower has in its output three pulses at spacings of 180° between them. Both the pulses modulate the beam intensity of the C.R.O. whose screen will show three spots (x axis is sufficiently amplified to remove off the screen the fourth spot corresponding to the 360° - pulse of the tachogenerator signal). Two spots, 'a' and 'b', correspond to the bus bar voltage, at a spacing of 180°, and one spot, 'c', corresponding to the shaft signal, the time base being synchronised to display a half cycle of the bus bar voltage. Spots 'a' and 'b' serve as 'marker' or 'reference' remaining steady at 180° apart and spot 'c' appearing in between varying in position along the x axis depending on the load angle. The phase shifter is adjusted such that 'c' would coincide with 'a' (or 'b') when the machine is on no load. This no load adjustment called 'Zeroing of the Oscilloscope', is achieved by adjusting the mechanical input of the machine such that the power transfer between the machine and the bus bars is zero. A precision wattmeter will help to achieve this adjustment.

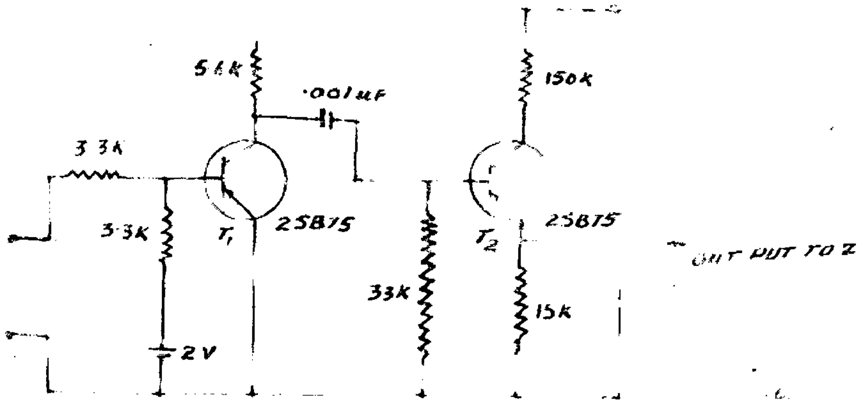

D.C. VOLTAGE 25 V.

TRANSISTOR PULSING CIRCUIT.

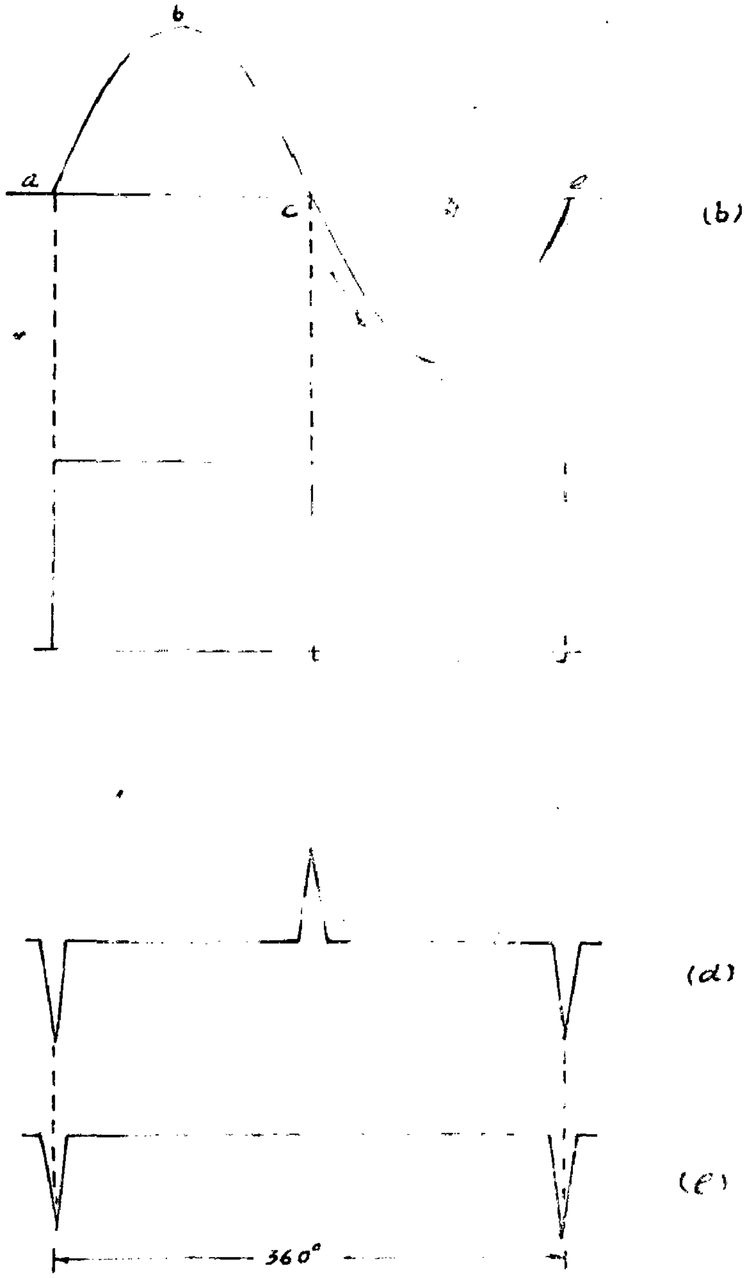

FIG. 7.4.

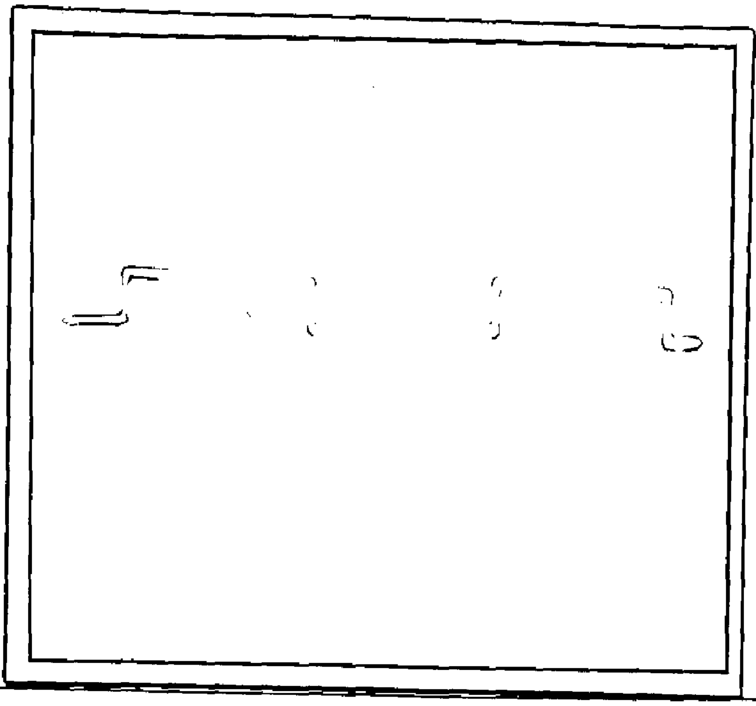

Oscillogram. Square wave output of transistor T_1 of Fig.7.4a.

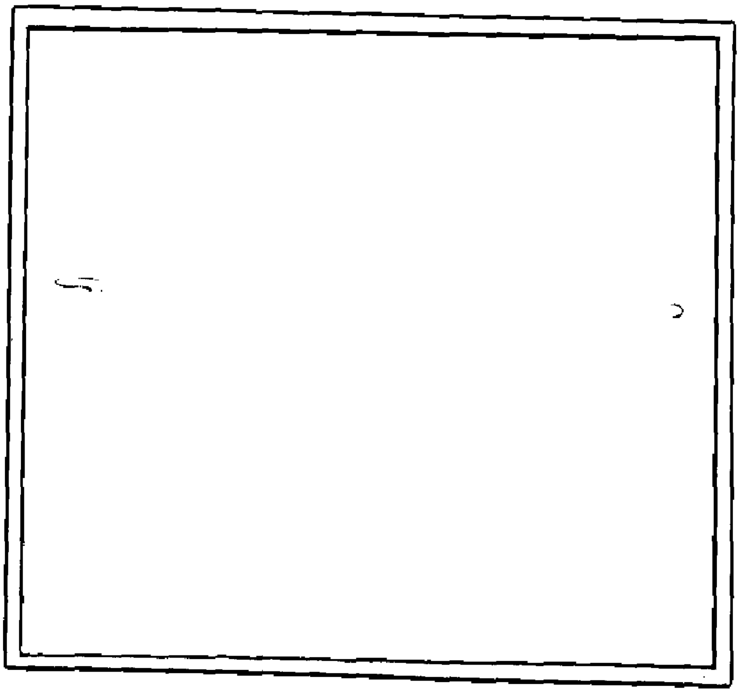

Oscillogram. Pulse formation after differentiation.

As the load angle varies the instantaneous position ofthe spot 'c' changes between 'a' and 'b' along the x axis and is a linear function of the load angle measured from 'a' (or 'b' depending upon with which spot zeroing was done). The Y plates remain unenergised and the load angle variation is recorded on a film moving along the Y axis at constant speed.

Pulsing circuit, Fig.(7.4a), merits a discussion. Transistor T_1 does not conduct during the positive half cycle 'abc' and conducts during the negative half cycle 'cde', Fig.(7.4b). The voltage across the transistor therefore rises to the supply value at 'a' and remains so till 'c' and from 'c' to 'e' drops down to almost zero. The input sinusoidal signal is thus converted into a square wave (Fig.7.4c) which is differentiated by C_1R_1 resulting in sharp pulses, Fig.(7.4d). Emitter-follower T_2 has in its output amplified pulses a cycle apart, Fig.(7.4e), the central one being eliminated. It being a positive pulse stops the pulse conduction of T_2 and the pulse voltage V_2 across the output load of 15K ohm is zero.

Reference signal is applied to pulser B, identical to pulser A, except that B is fed through a bridge rectifier, Fig.(7.5a). Stages of pulse formation are shown in Fig.(7.5 b,c,d). Though the output of T_1 fed through a rectifier appears like pulses, their widths at the points in question are considerably large. To sharpen, therefore, and accentuate them it is necessary to differentiate and pass them through an emitter-follower as before.

One difficulty likely to be encountered invariably is in the choice of the four bridge elements. Owing to their non matching and non identical characteristics the rectified wave is likely to be somewhat as shown in Fig.(7.6a), with the tip 'f' below the base line. As the phase shifter is rotated 'f' moves horizontally

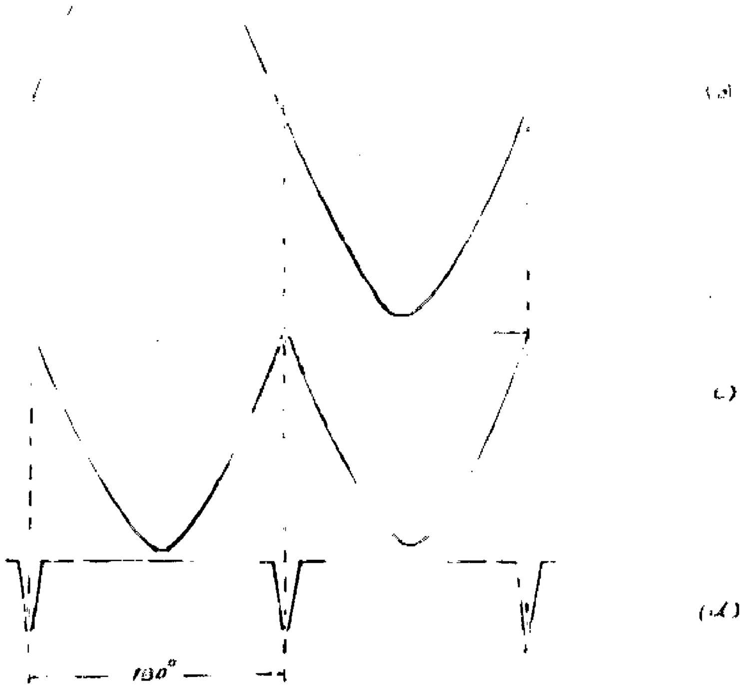

FIG 1.5

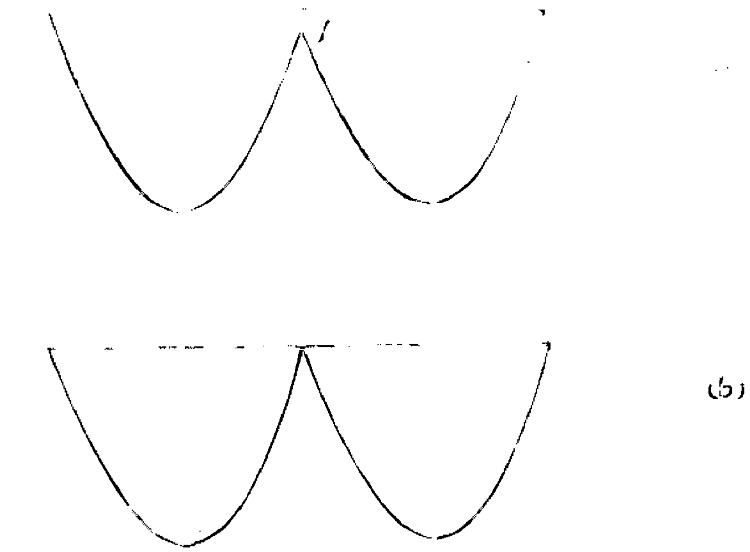

FIG 1.6 (a) WITHOUT BIAS
(b) WITH BIAS

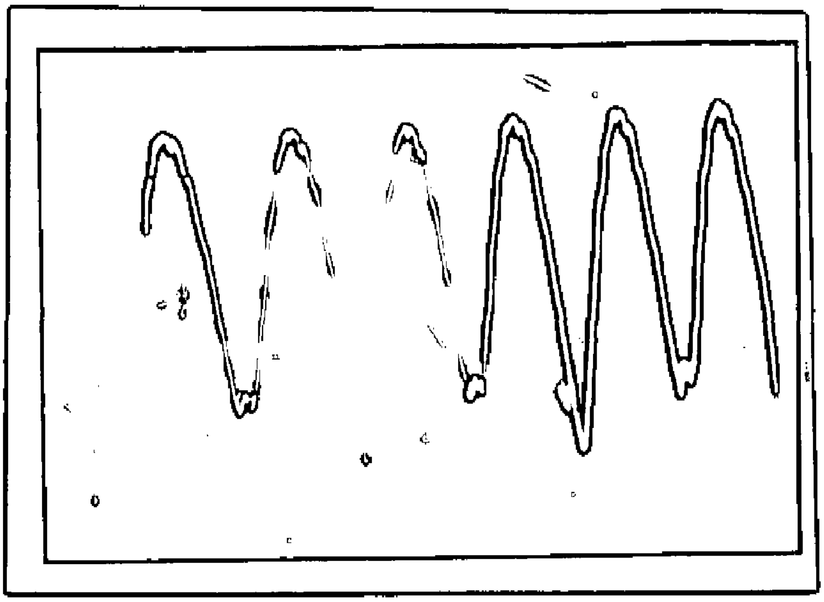

Oscillogram. Full wave bridge rectifier output of Fig.7.5a with diodes of nonmatching characteristics; without biasing.

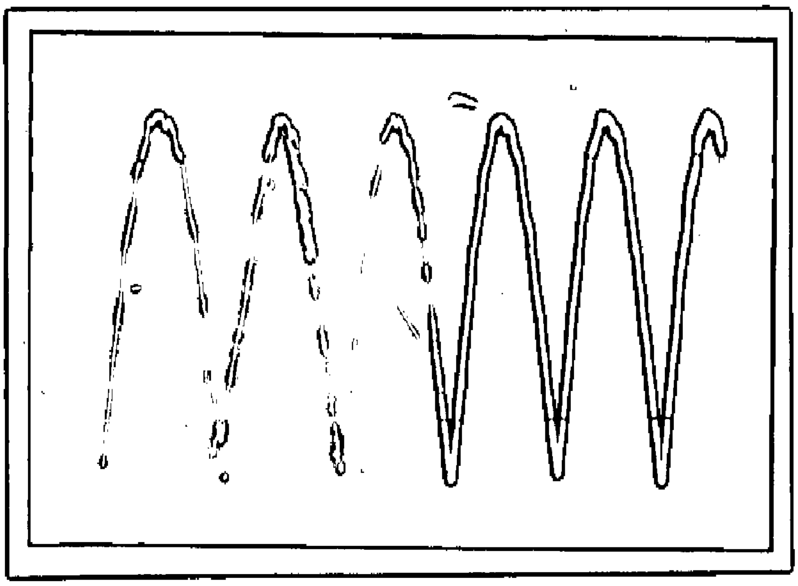

Oscillogram. Full wave bridge rectifier output of Fig.7.5 with diodes of non-matching characteristics with and slightly upwards and downwards too; the pulse, therefore, corresponding to 'f' (the 180° point) appears and disappears at different phase shifter positions. This baffling difficulty can be overcome by a careful choice of identical diodes. This may not always be possible and a remedy is to be sought otherwise. A suitable reverse-biasing of T_1 will eliminate this trouble, Fig.(7.6b). A 2 volts battery through a 3.3K ohm resistor has accomplished the desired result in the present work. Should excessive biasing become necessary this method should not be resorted to, because it would then reduce the clearance between the reference spots to less than 180°. In such cases matching diodes consitute the only solution.

Thus the angle recording device developed here is simple in construction and application.

CHAPTER VIII

DESIGN, CONSTRUCTION AND CALIBRATION OF A LOW FREQUENCY OSCILLATION GENERATING DEVICE

Any experimental investigation concerning large oscillations in a synchronous machine needs a device to produce them at will at the desired frequency and having the desired waveform. The problem at hand is to produce sinusoidal oscillations of the load angle at low frequency varying between 0.5 cps to 2.5 cps. The technique could be either the synchronous machine should drive a load whose torque has a cyclic irregularity or it should be driven by a drive whose torque varies cyclically at the specified frequency. Obviously the latter is easier and aminable to control, particularly if the drive be a d.c. motor. Between the two alternatives of armature or field control the latter is simpler and calls for less elaborate, low-power equipment. A changing field produces changes in the driving torque and hence changes in the load angle which in turn affect the torque.

At first thought it would seem that a low frequency sinusoidal voltage from the slip rings of an induction motor superimposed on the main field would answer the situation. But this voltage is about 2 to 4 volts and has a frequency about a cycle per sec. at no load. (The frequency can be increased by increasing the load on the motor slightly.) The voltage being too small to be effective in the field circuit having generally a high resistance (about 330 ohms in the present case) needs to be stepped up. The frequency being too low no transformer would be available to achieve this.

A useful source can be found in a rotary converter driven in a direction opposite to the rotating magnetic field by a d.c. motor at speeds other than the synchronous speed while supplying its armature with three phase a.c. line voltages at its slip rings. Whereas the magnitude of the voltage obtainable at the d.c. brushes depends upon the speed of the armature relative to the rotating field and has a constant value since the relative speed is always synchronous, the frequency of that voltage depends upon the actual speed of the field in space. Thus a considerably large voltage is obtainable at the desired frequency. But the system is elaborate and a d.c. machine of suitable capacity to drive the converter will be needed. In laboratories of today it may be hard to find a rotary converter since it has become obsolete commercially and has retained academic interest only.

A device, therefore, that does not demand any special machinery would evidently be a welcome feature. The most elementary idea of converting rotary motion into reciprocatory motion is utilized in varying sinusoidally a rheostat series-connected in the field circuit of the driving d.c. motor, the field winding being separately excited. Photograph, 8.1a shows the unit and Fig.8.1b shows its schematic. A 1 h.p. shunt motor mounted on a pedestal drives through a 2" diameter pulley and a V belt (A 46)a 12" diameter disc mounted on a shaft supported on two bearings. This shaft drives a $\frac{3}{8}$" x 10" diameter plate carrying eccentrically a rod connected to the brush of a 350 ohm rheostat through a knuckle joint. As the motor runs the rheostat brush performs oscillatory motion and the field current through it varies sinusoidally. The frequency of oscillation can be controlled very accurately through a potential divider supplying the armature under constant field. The amplitude of oscillation can be controlled by fixing the eccentric rod on the circular driving plate at different radial points. A counter

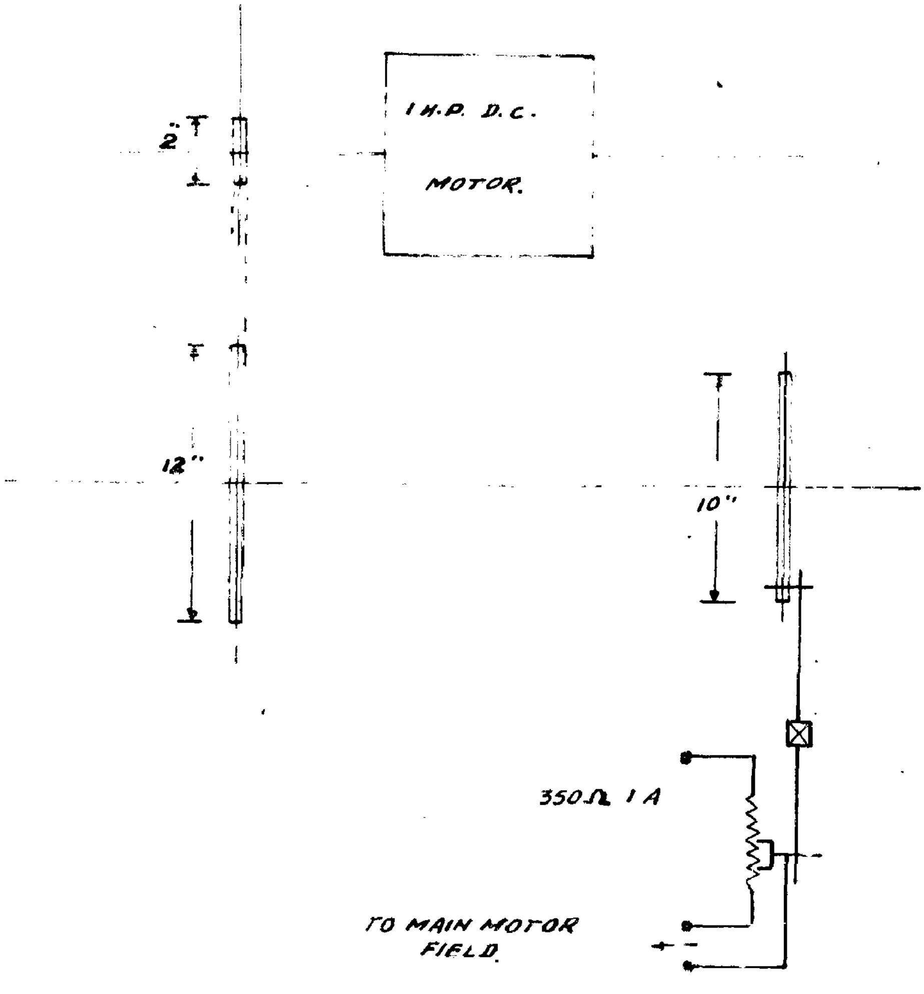

FIG. 8.1(b) SCHEMATIC OF THE LOW FREQUENCY OSCILLATION GENERATING DEVICE.

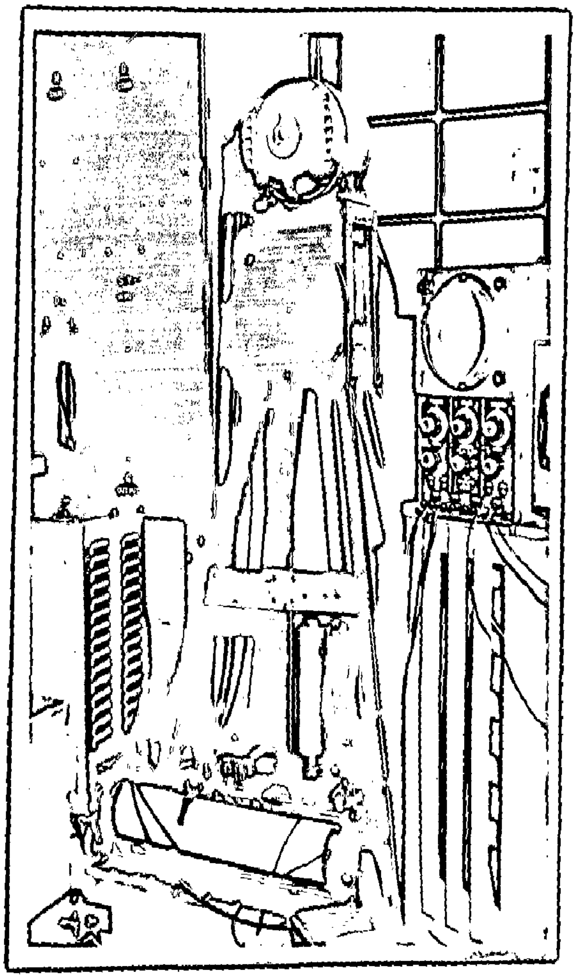

8.1a. Mechanical system for producing large oscillations.

weight is put to balance the motion so that the upward and downward. travels of the brush take the same time. The frequency is checked approximately by forming Lissajous patterns on an oscilloscope whose X- plates are energised from a function generator giving sinusoidal voltages of the required low frequency and the Y-plates by a signal from the field circuit. Precise setting is achieved with the help of a stop watch by counting the frequency as the cathode ray beam moves along the Y-axis with the time base switched off.

A singular disadvantage of the mechanical system is its two dead bands.

CHAPTER IX

MEASUREMENT.

9.1. Using the set up described in Chapter V conditions assumed in Chapter IV are experimentally produced. The line current from the bus bars is limited to about .5 p.u. with the help of the external reactor. Oscillograms of torque, current and load angle are recorded such that the first two are on the same film using a double beam oscilloscope and the third one on another film using an oscilloscope with Z modulation.

9.2. DETAILS OF SET UP AND SPECIFICATIONS:

External reactance, x_e 1.35 p.u.

Zeroing apparatus:

Precision wattmeter,

Low p.f., 230V, 10A, connected in one phase.

Phase shifter, 3 phase 400V, 5KVA, 50 cps Δ/Y

Rotor Position Pick-up: Tachogenerator, 4 poles; its output was found to be free from harmonics.

Oscilloscope:

'COSSOR' DUAL BEAM for torque and current recording.

'DUOSCOPE' DOUBLE BEAM, high grade with Z modulation operating on cathode and intensity control on grid for load angle recording.

'DUMONT' SINGLE BEAM for checking the low frequency oscillation

Cameras:

'COSSOR', 2 Nos.

Film:

OR WO, 35 mm, 400 ASA, Ultra fine grain,

Recording Speed: 1 inch per sec.

9.3. For the purpose of verification the case of 2 cps oscillation is chosen. Nevertheless, as could be seen from the oscillograms, it is only this case where the effect of dead band of the mechanical reciprocatory system is effectively swamped (by the inertia of the rotating masses). The torque signal record, though fairly satisfactory qualitatively, stands to no avail for quantitative measurement. Therefore a verification of the current signal record only is done.

9.4. The different components of d,q axis currents calculated in Chapter IV pertain to the case when the machine is connected directly to the infinite bus. As a matter of necessity and inevitability series reactors have been used between the machine and the bus bars during the experimentation. Therefore, transfer reactance $x_{d(q)t}$, operational impedances, $x_{d(q)}(jk)$, and the currents $i_{d(q)s(c)n}$ are recalculated for the case of $\frac{K}{2\pi} = 2$ cps.

$x_{dt} = 2.43$ $\qquad$ $x_{qt} = 1.798$

$x_d(jk) = 1.58 - j.0542$ $\qquad$ $x_q(jk) = 1.793 - j.044$

$x_d(j2k) = 1.577 - j.0309$ $\qquad$ $x_q(j2k) = 1.775 - j.0825$

$x_d(j3k) = 1.554 - j.0216$ $\qquad$ $x_q(j3k) = 1.687 - j.112$

<u>Currents</u>

$i_{do} = \sqrt{2} \times .16$ $\qquad$ $i_{qo} = \sqrt{2} \times .269$

$i_{ds1} = \sqrt{2} \times .109$ $\qquad$ $i_{qs1} = \sqrt{2} \times .166$

$i_{ds2} = \sqrt{2} \times .000326$ $\qquad$ $i_{qs2} = -\sqrt{2} \times .000398$

$i_{ds3} = \sqrt{2} \times .00128$ $\qquad$ $i_{qs3} = \sqrt{2} \times .00206$

$i_{dc1} = \sqrt{2} \times .00373$ $\qquad$ $i_{qc1} = \sqrt{2} \times .0041$

$i_{dc2} = -\sqrt{2} \times .0167$ $\qquad$ $i_{qc2} = \sqrt{2} \times .00855$

$i_{dc3} = \sqrt{2} \times .0000176$ $\qquad$ $i_{qc3} = \sqrt{2} \times .000136$

The instantaneous amplitude of the armature current in each phase is given by

$$|i_a| = \{(i_{do}+i_{ds1}\sin kt + i_{dc1}\cos kt+\ldots\ldots)^2+(i_{qo}+i_{qs1}\sin kt+ i_{qc1}\cos kt+\ldots\ldots)^2\}^{\frac{1}{2}} \quad \ldots \quad \ldots(71)$$

Table II shows the values of $|i_a|$ calculated over a cycle using equation (71) against its values obtained by measurements from the oscillographic record of the armature current. Fig.9.1 is a graphical representation of Table II, plotting being done to two significant figures.

TABLE II

$\frac{K}{2\pi} = 2$ cps

$Kt = 4\pi t$	$\|i_a\|$ Calculated from eqn.71	$\|i_a\|$ measured from the oscillogram
0^o	.453	.533
30^o	.595	.629
60^o	.695	.695
90^o	.706	.706
120^o	.680	.680
150^o	.580	.560
180^o	.440	.440
210^o	.298	.273
240^o	.198	.134
270^o	.164	.124
300^o	.198	.177
330^o	.312	.297
360^o	.453	.425

Table III is drawn up to show the torque variation as a function of time as calculated from the torque terms in Table I, Page 26 for the case $\frac{K}{2\pi}$ = 2 cps the machine being connected

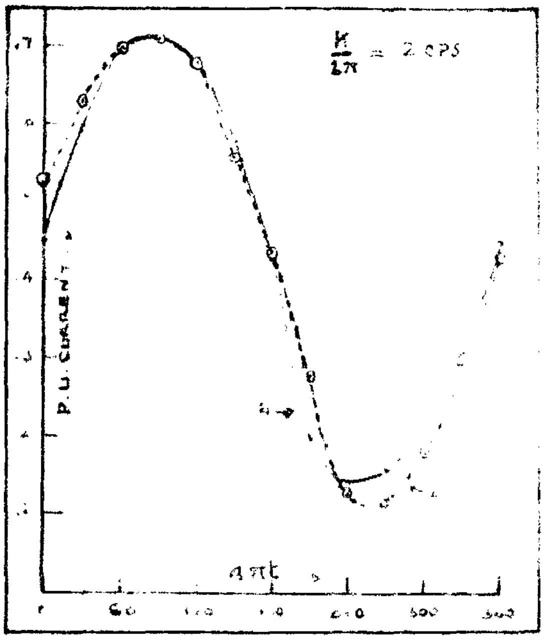

Fig. 9.1 Current waveforms
a ——— Calculated
b - - - - Test

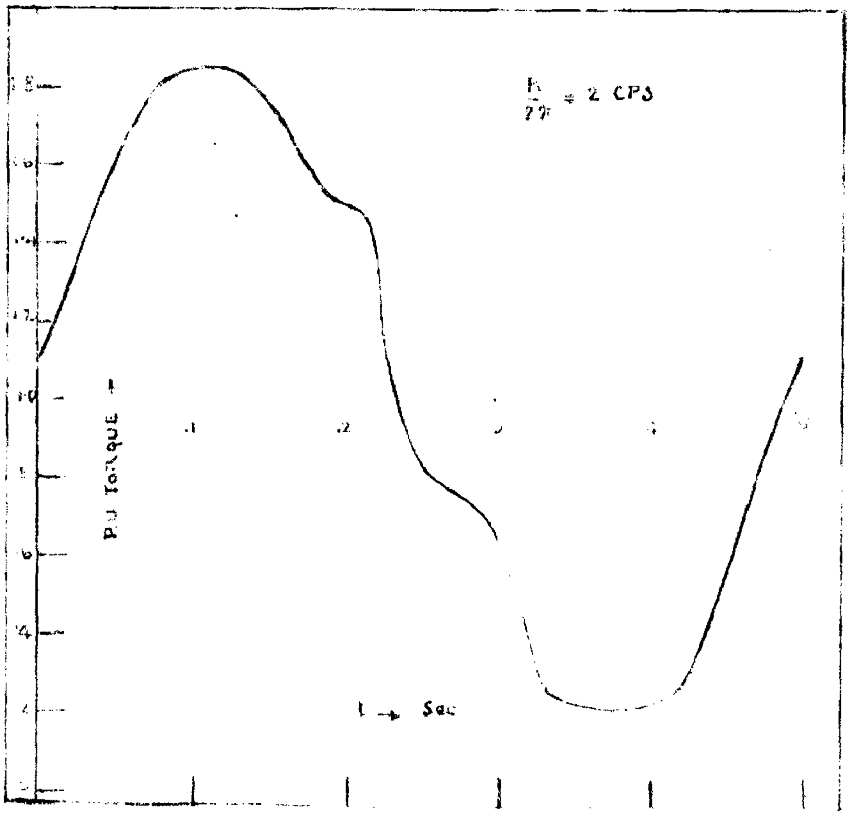

Fig. 9.2. Calculated Torque Variation.

Oscillogram. Torque oscillation

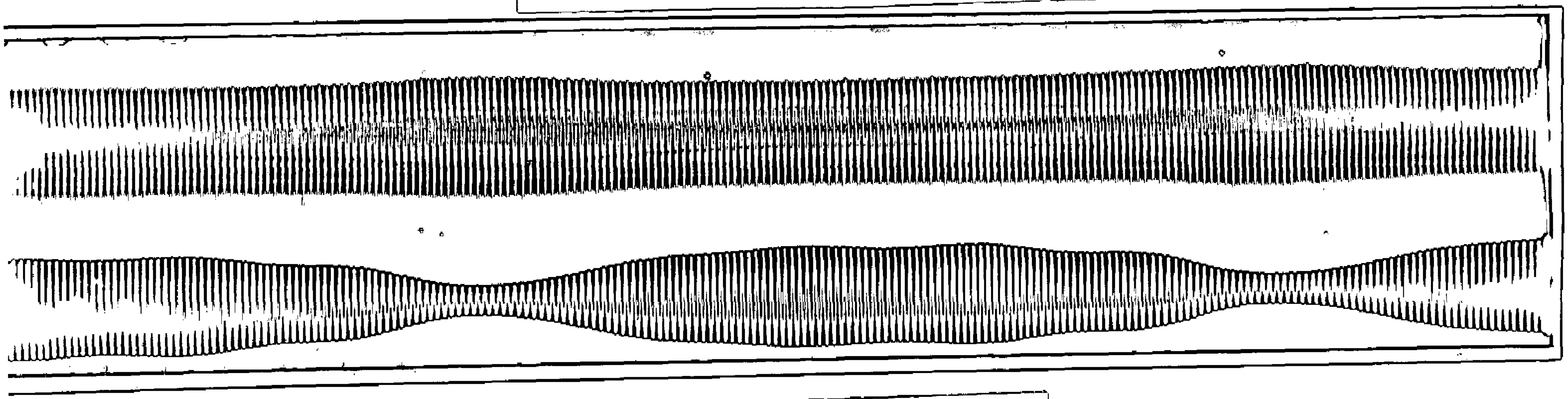

Oscillogram. Current Oscillation

Oscillogram. Torque oscillation

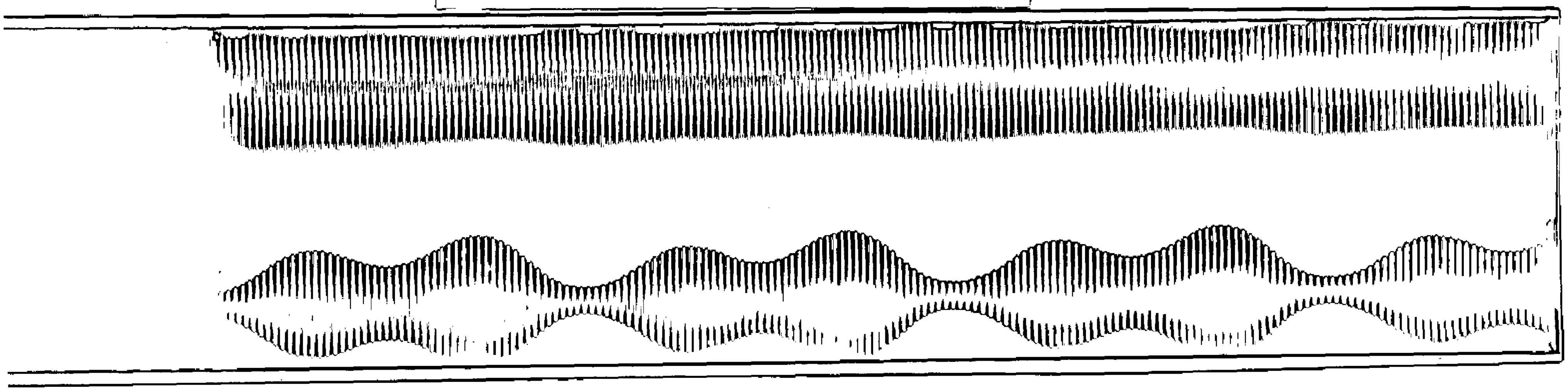

Oscillogram. Current Oscillation

Oscillogram. Torque oscillation

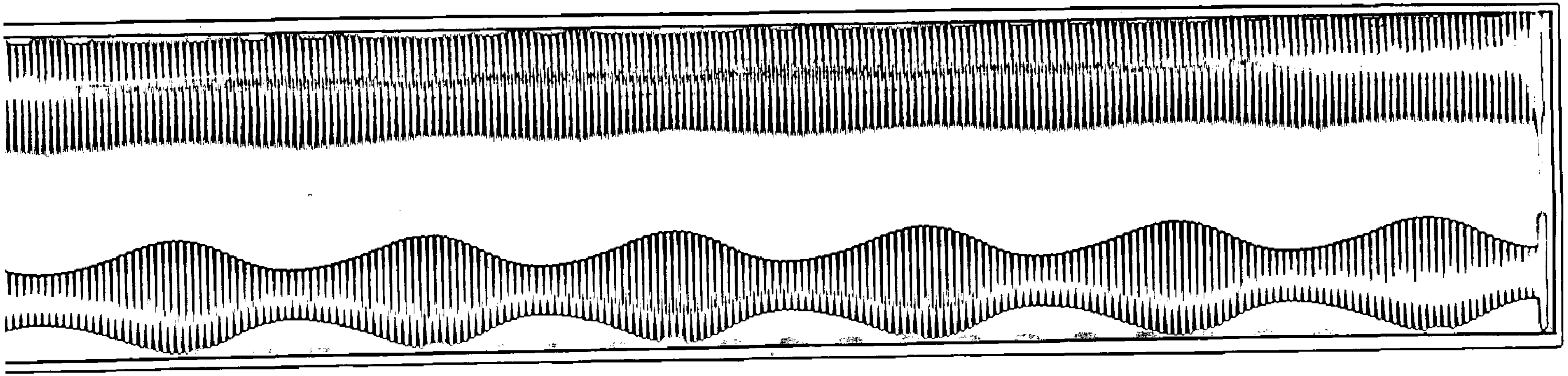

Oscillogram. Current Oscillation

Oscillogram. Torque oscillation

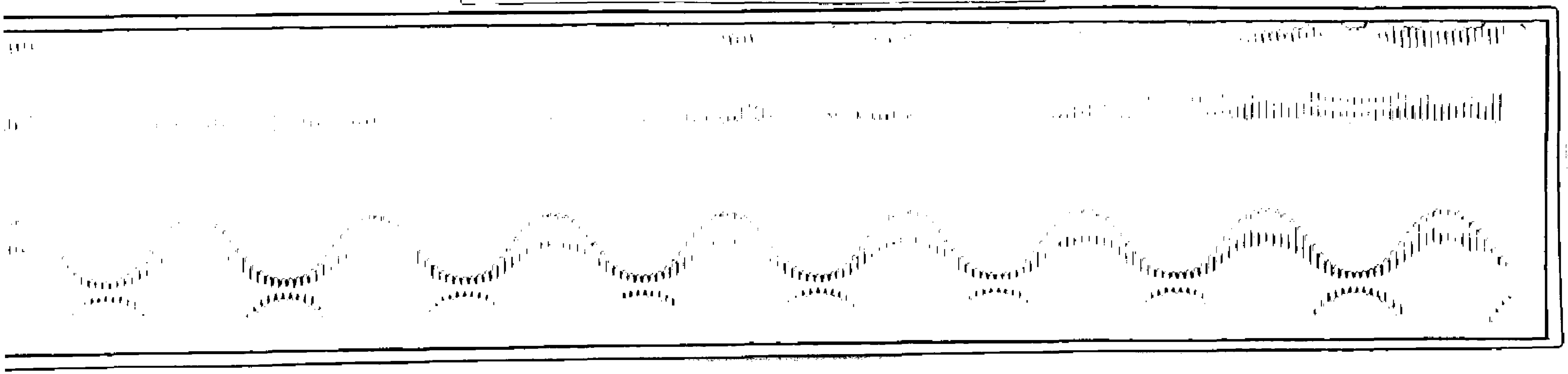

Oscillogram. Current Oscillation

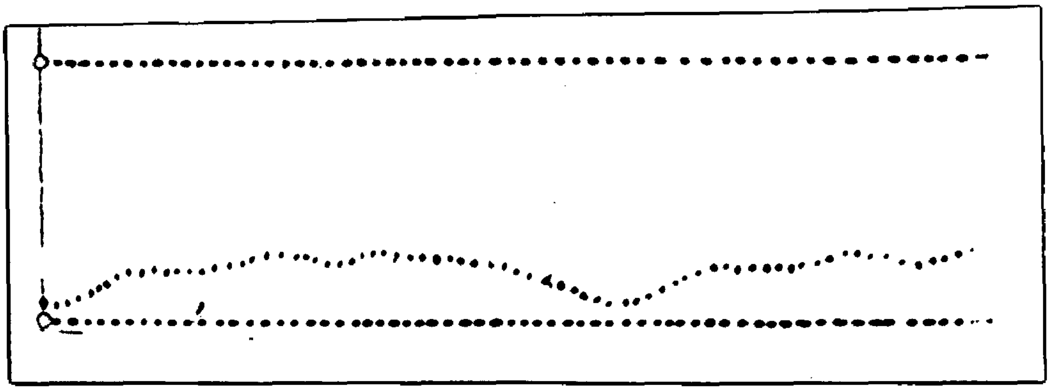

Oscillogram. Load angle Oscillation, at $\frac{K}{2\pi} = 0.5$

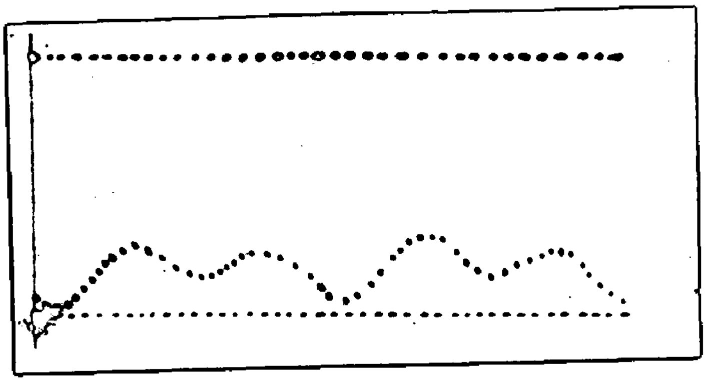

Oscillogram. Load Angle Oscillation, at $\frac{K}{2\pi} = 1.0$

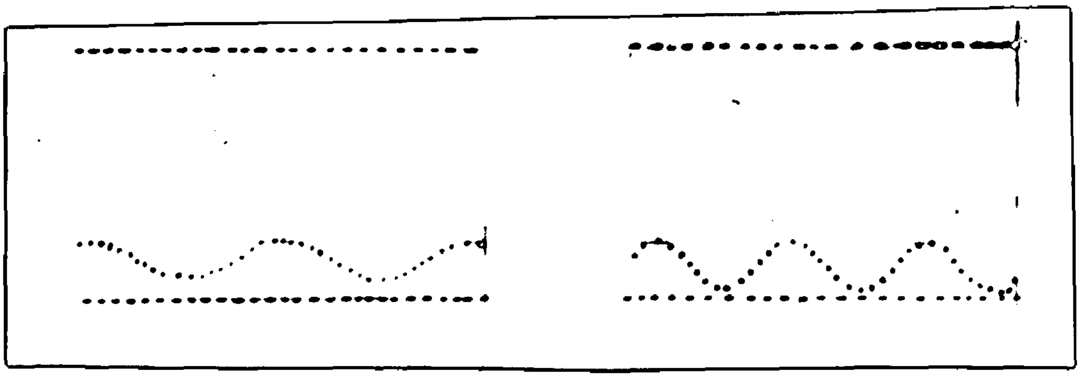

lo ram. Load An le Oscillation, $\frac{}{\pi} = 1.5$

Oscillogram. Load Angle Oscillation, at $\frac{K}{2\pi} = 2.0$

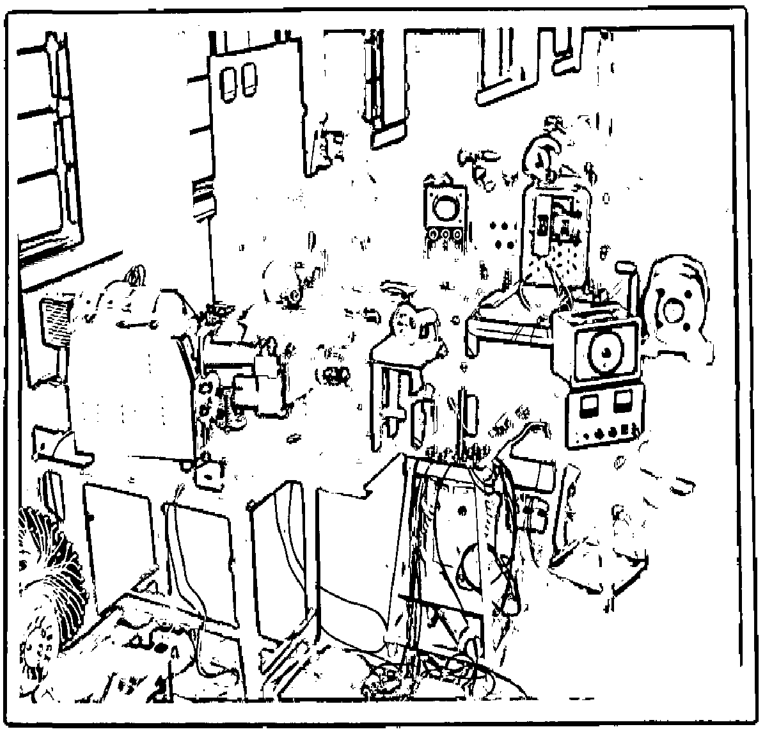

A comprehensive view of the experimental set-up

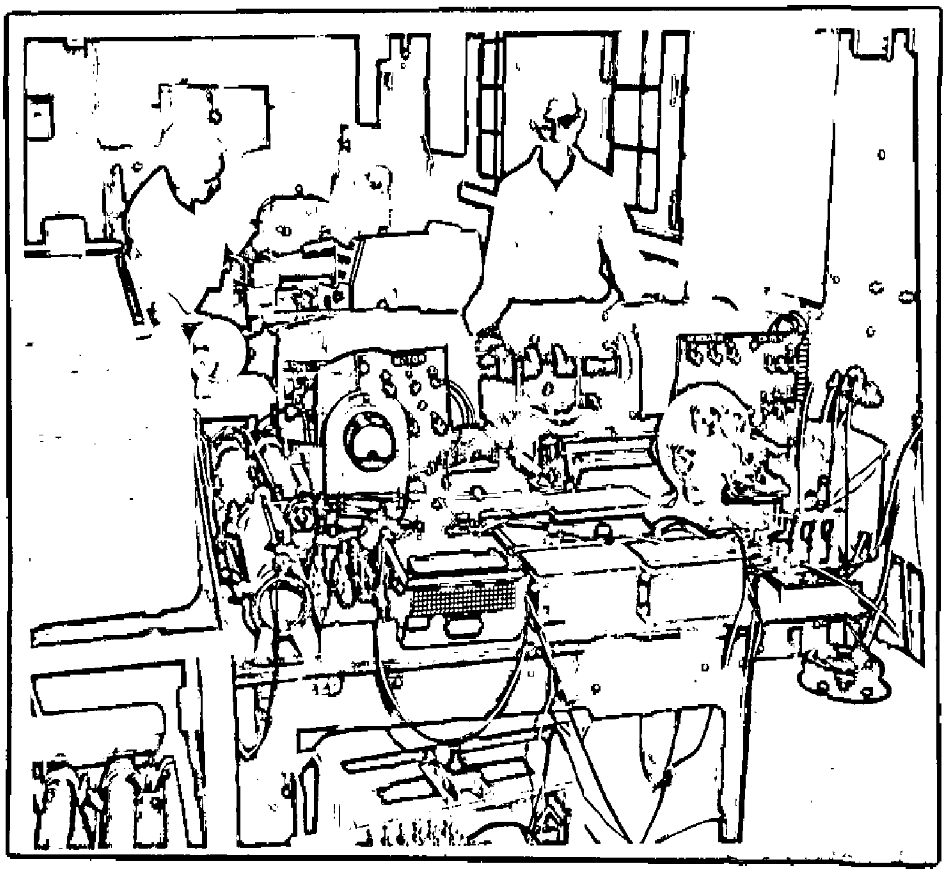

Another view of the set-up showing the torquemeter interposed between the driving and the driven machines.

directly to the infinite bus. Fig.(9.2) is a torque-time plot of table III.

TABLE III

$$\frac{K}{2\pi} = 2 \text{ cps}$$

t sec.	T P.U.	t sec.	T P.U.
.000	1.236	.292	.832
.041	1.672	.333	.383
.083	1.948	.375	.344
.125	1.984	.417	.379
.167	1.777	.458	.393
.186	1.645	.5	1.236
.208	1.635		
.25	.956		

9.5. As a matter of interest the behaviour of the torque meter is studied using the calibration circuit of Fig.(9.3). The milliammeter reading is recorded for different values of the steady state transmitted torque. The driving d.c. motor is calibrated and table IV is prepared showing values of torque transmitted in ft.lbs., against the milliammeter reading. Fig.(9.4) represents table IV graphically.

TABLE IV

Transmitted torque lbs.ft.	Response of the torque meter m.A.	Load condition of Synch. machine
1.5	.4	No load
7.7	.3	20% load
9.8	.2	23% load
11.9	.1	30% load

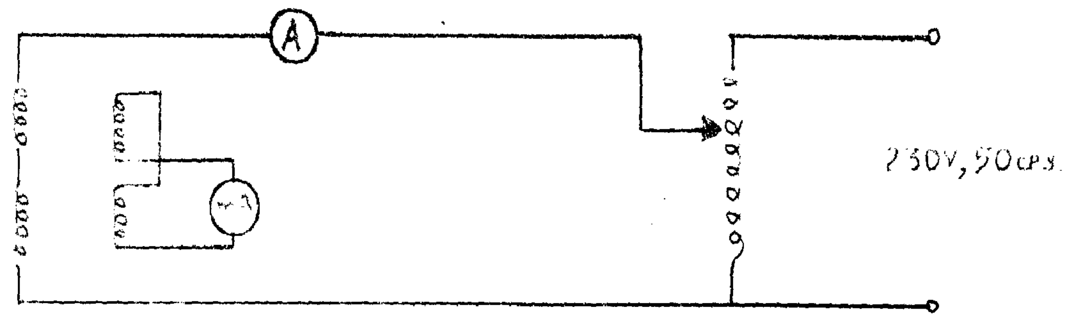

Fig. 9 5. Calibration of Torque Meter.

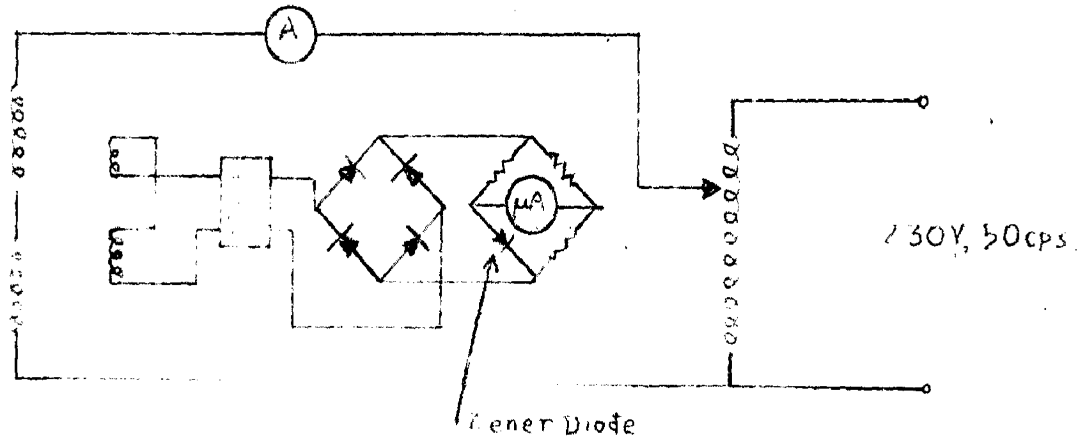

Fig. 9 5.

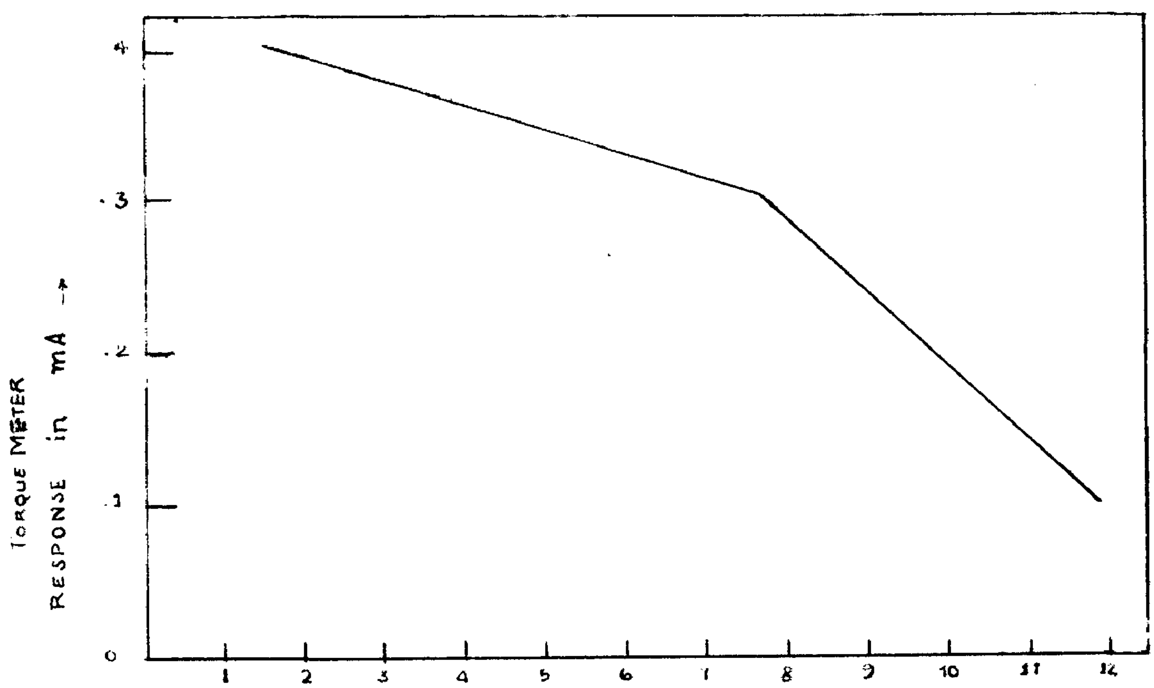

Fig. 9.4 Calibration Curve Of Torque Meter

It is observed that while the behaviour of the torque meter is linear above 20% loading, it is arbitrary below 20%.

A better method of calibration would be to amplify the torquemeter signal, to rectify and smooth it out and to supply it to a null detecting bridge carrying a zener diode in one of its arms, Fig.(9.5). When no torque is transmitted the bridge is balanced. The amount of unbalance detected on a micro-ammeter is in direct proportion of the torque transmitted.

CHAPTER X

CONCLUSION.

The numerical analysis and the experimental technique presented in this dissertation concerning a large non-linear oscillation in a synchronous machine have proved conclusively the validity and efficacy of the large oscillation theory which is derived by applying rigorous mathematics to Park's equations. No ambiguity of any kind has been encountered in the process and only those assumptions usually justified and made by other authors are made here also. With the limitations of the instruments and their accuracies the close agreement between the calculated and the test wave-forms is quite encouraging. Except at two points, the departure of the test wave varies from 6.7% to zero.

It should be interesting to study the case of 'self oscillations' in the light of the large oscillation theory. Suitable experimental technique can be developed to produce self maintained oscillations by inserting more resistance between the synchronous machine and the bus bars. Also further work is possible by taking into consideration the effect of voltage regulators.

The torque meter designed and developed in this connection, though enjoys certain advantages of being brush-less and sliprings-less, has a poor response which constitutes the glaring inadequacy for a quantitative instrument. It is useful for qualitative observations but only this does not justify the labour involved in its making. However improvement on this design is possible by making the toothed rings on a milling machine. To use the bridge output of Fig.(9.5) as the torque meter signal for the C.R.O. for recording torque variations should be a better method.

The load angle meter developed here can be used with any machine for both steady state and transient studies. It is useful in determining the machine swing curves directly and accurately.

The mechanical reciprocating system used here, though can produce absolutely sinusoidal variations in the field current, has the serious disadvantage of two dead bands which cannot be eliminated. These produce unwanted oscillations in the torque and current and hence in the speed of the local driving motor. These rider frequencies become felt at low frequency settings and are ineffective at 2 cps and higher. Mechanical smoothing by a flywheel will reduce the trouble considerably. A rotary converter driven by a d.c. motor offers a more favourable solution.

B_I_B_L_I_O_G_R_A_P_H_Y.

1. C.A. Nickle and C.A. Pierce, "Stability of Synchronous Machine, Effect of Armature Resistance". Trans.A.I.E.E., Vol.49,1930, p.338.

2. C.E. Wagner, 'Effect of Armature Resistance on Hunting', Trans. A.I.E.E.,Vol.49, 1930, p.1011.

3. W.J. Gibbs, 'Tensors in Electrical Machine Theory', Chapman Hall, 1951.

4. B. Adkins, 'The General Theory of Electrical Machine', Chapman Hall Ltd., 1951.

5. R.N. Sudan, V.V. Manohar and B. Adkins, 'Measurement of Transient Load Angle in Model Synchronous Machine', Proc.I.E.E., Vol.107, Part A, 1960, p.51.

6. P. Mukhopadhyay, 'A note on the Determination of Synchronous Reactances of a Salient Pole Machine', International Journal of Electrical Engineering Education, Vol.6, 1968, p.87.

7. Narayan Prasad, 'A Torque Recording Device'. M.E. Thesis, University of Roorkee, 1965.

8. Sujoy Basu and P. Mukherji, 'On Large Oscillation of Synchronous Machine'. Journal of Technology, Vol.IX, No.1, 1964, p.17.

9. C. Concordia, 'The Synchronous Machine, Theory and Performance'. John Wiley.

10. M.G. Say. 'Performance and Design of Alternating Current Machines' Sir Isaac Pitman & Sons.Ltd.,1958,p.648.

11. B. Adkins, 'The Application of the Frequency Response Method in Electrical Machines', Proc.I.E.E., Monograph No.178, May 1956.

12. B.C. Carter and J.F. Shannon, 'Measurement of Displacement and Strain by Capacity Methods'. Proc. I.M.E.,Vol.152, No.2, 1945, p.215.

13. C.H.G. Mills, 'A Capacitance Type Torque Meter', Journal of Scientific Instruments, Vol.25, 1948, p.151.

14. Y.C. Sood, 'Design, Fabrication and Testing of a Strain gauge Torque-meter'. M.E. Thesis, 1963, Mech.Dept., University of Roorkee, Roorkee.

15. C.R. Arthur, 'Bonded wire gauge Torquemeter', Experimental Stress Analysis, Vol.1, No.2, 1943, p.68.

16. J.C. Enslin, 'The Method of Using Microwaves for Measuring Small Displacements and a Torque meter using this principle', Proc.I.E.E., March 1954, Vol.101, Part B, p.522.

17. B.F. Langer, 'The Magnetic-coupled Torquemeter'. Experimental Stress Analysis, Vol.2, No.2, 1945, p.11.

18. S.M. Peeran and B.L. Mathur, 'Measurement of Synchronous Machine Power Angle', Journal of the Inst.of Engineers (India), Vol. XLVI, No.8, Part El., April.1966, p.270.

19. E.B. Powell and M.E. Harper, 'Generator Rotor Angle Measurement by Stroboscopic Means', Proc.I.E.E., Vol.105, Part A, 1958, p.609.,

20. H. Holloway, 'An experimental Technique for Direct Recording of Machine Swing Curves', International Journal of Electrical Engineering Education, Vol.2, 1964, p.203.

21. J.N. Prewett, 'A method of Measuring and Displaying Generator Rotor Angle', Proc.I.E.E. Vol.105, Part A, 1958, p.613.

22. W.Charlton, 'Measurement of Synchronous Machine Rotor Angle', International Journal of Electrical Engineering Education, Vol.2, 1964, p.203.

23. T.H. Mason and P.D. Aylett and F.M. Birch, 'Turbo Generator Behaviour in Abnormal Operating Conditions', Proc.I.E.E., Vol.107, Part A, 1960, p.307.

24. M.S. Berde and R.C. Paul, 'A Phase Angle Meter for the Study of Swinging Curves of Synchronous Machines in the Study of System Stability'. Journal of the Institution of Engineers (India), Vol.43, No.8, Part El.4, April 1963, p.157.

25. V.A. Kinitsky, 'Measurement of Rotor Angle Displacement on Synchronous Machine', Trans. A.I.E.E., Vol.77, Part III, 1958, p.349.

26. S.K. Murthy and S.L. Surana, 'A New Method of Measuring the Load Angle of Synchronous Machine', Journal of the Institution of Engineers (India), Vol.48, No.8, Part E14, April 1968, p.552.

27. S.B. Crary, 'Power System Stability', John Wiley, Vol. 2, 'Transient Stability', 1947.